

Synoptic systems: Flow-dependent and ensemble predictability

*Federico Grazzini ARPA-SIMC, Bologna, Italy
fgrazzini@arpa.emr.it*

Thanks to Stefano Tibaldi and Valerio Lucarini for useful discussions and suggestions. Many thanks also to Alain Bataille for his assistance in producing some maps.

Outline

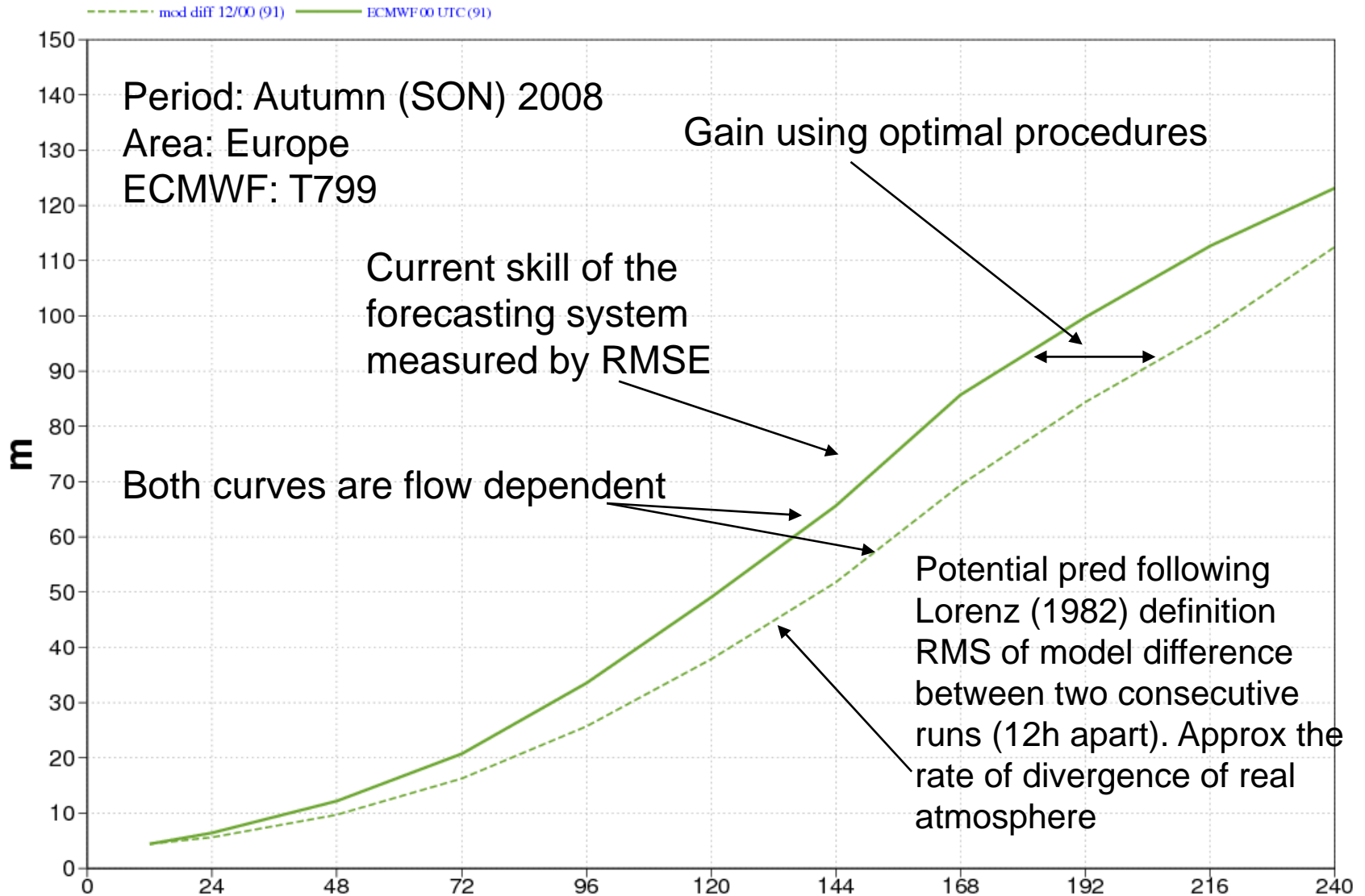
- Phenomenological approach to predictability
- Review and evidences of flow dependent *predictability*
- Evolution of predictive skill associated with a particular flow type
- Rossby Wave Packet (RWP) propagation and predictability

Predictability definitions

Lorenz, 2006

- *Predictability or Intrinsic Predictability*: the extent to which prediction is possible using an optimal procedure. This represents an upper limit and it is essentially determined by the stability properties of the atmospheric flow.
- *Practical predictability or predictive skill or forecast accuracy*: the extent to which we are currently able to predict with current procedures

A visual illustration



Is forecast accuracy (or predictive skill) dependent on the flow ? A brief review

Skill sensitivity to flow type in IC....wave train

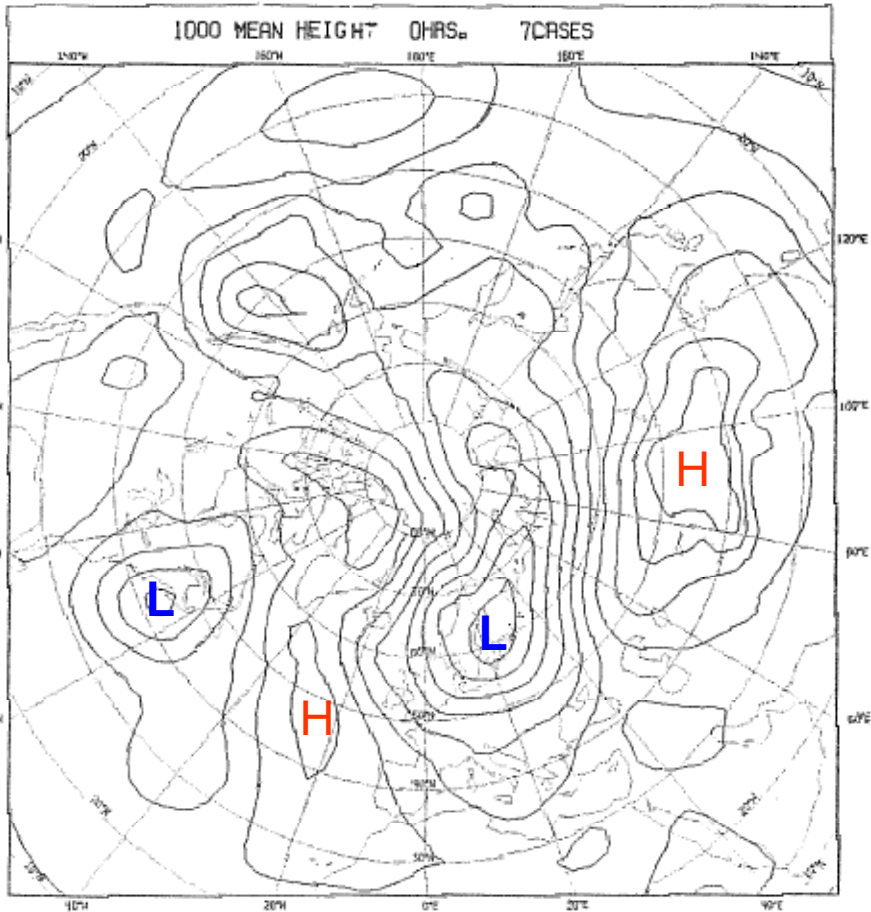


Fig. 3.2 Mean analysis, 3 - 9 December 1981

GRØNAAS, 1982

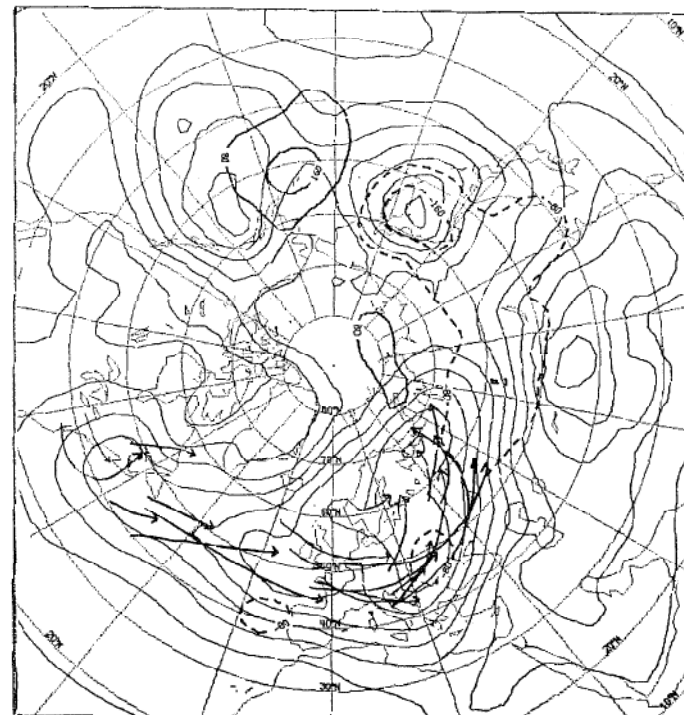


Fig. 3.3a
Mean day 7
1000mb height
forecast from
the period
3-9 December 1981

Dashed lines
mean errors

Forecasted low
tracks from
day 5 to day 7
in the European/
Atlantic area

Mean 500mb anom.
correlation,
European area:
day 3 .93
day 5 .86
day 7 .82

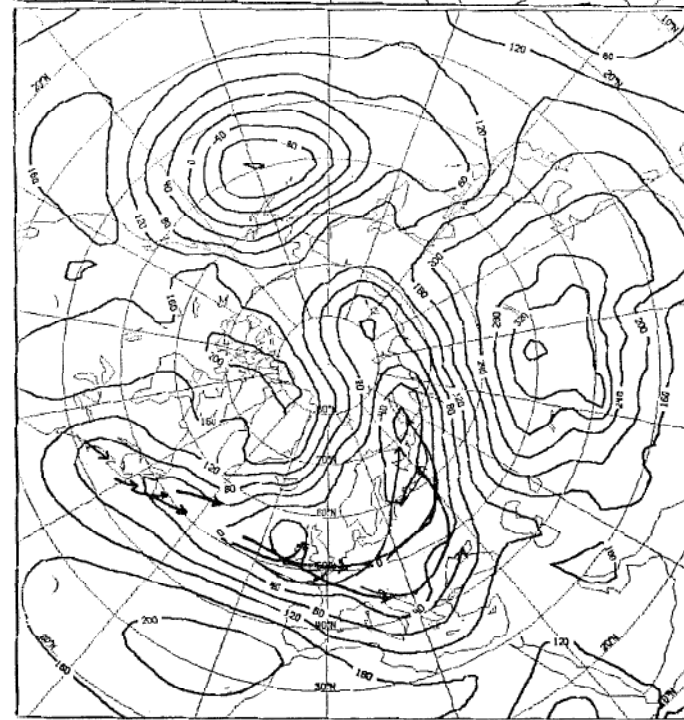


Fig. 3.3b
Mean verification
1000mb height
analysis

Low tracks
for the
European/
Atlantic area

Skill sensitivity to flow type in IC....zonal

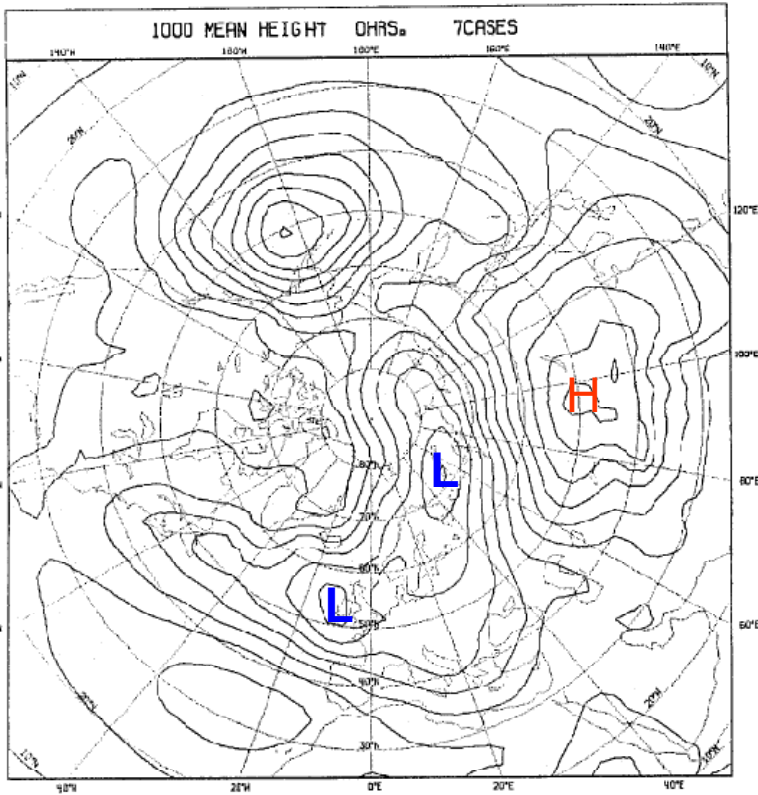


Fig. 3.4
Mean analysis
for the period
11-17 Dec. 1981

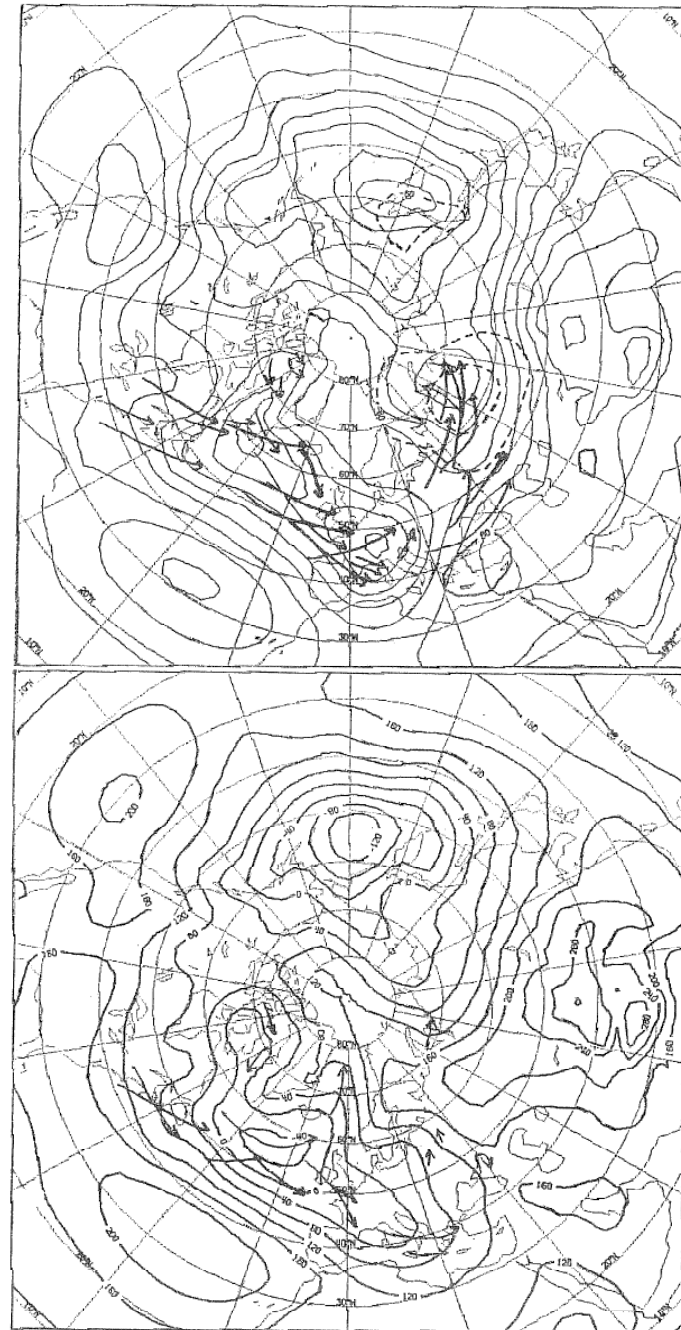


Fig. 3.5a
Mean day 7
1000mb height
forecast from
the period
11-17 Dec. 1981

Dashed lines
mean errors

Forecasted low
tracks from
day 5 to day 7
in the European/
Atlantic area

Mean 500mb anom.
correlation,
European area:
day 3 .85
day 5 .56
day 7 .35

Fig. 3.5b
Mean verification
1000mb height
analysis

Low tracks
for the
European/
Atlantic area

GRØNAAS, 1982

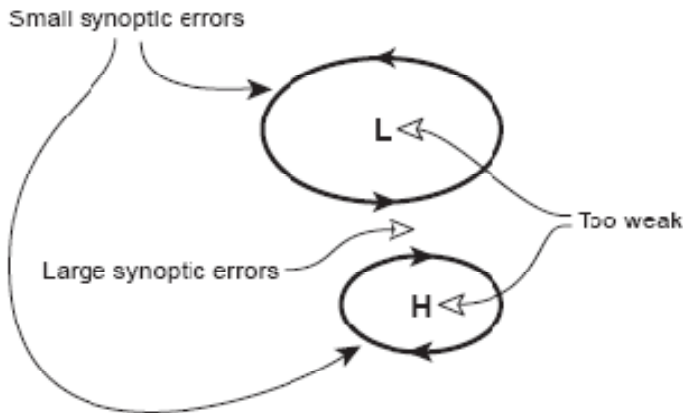
Sensitivity to blocking and PNA

- Palmer et al. (1989) found a strong correlation between PNA patterns and medium range forecast skill
- Tibaldi and Molteni (1990) investigated the predictability of blocking, finding that blocking frequency was severely underestimated in medium-range forecasts; the model was reasonably skilful when blocking was already present in the initial conditions. Blocking onset was very poorly represented if it occurred more than a few days into the forecast

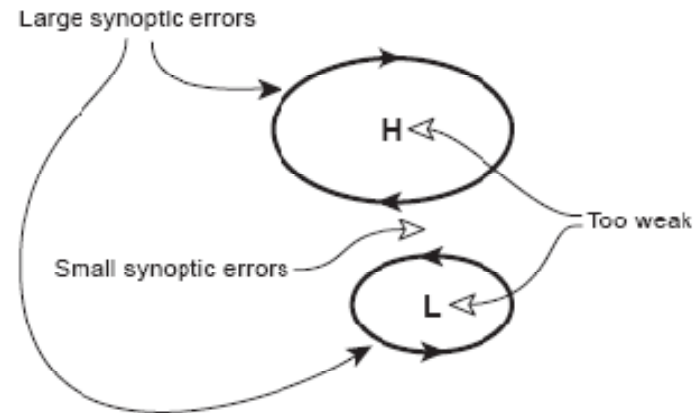
Sensitivity to NAO conditions

Ferranti et al., 2002

NAO+



NAO-



In a zonal like flow condition error growth is fast and affects more synoptic scale systems developing in a baroclinic flow, in more undulated flow type error growth is slower and errors are affecting more the large scale.

Following indications from diagnostics many changes have been introduced with a beneficial effect on model accuracy

ECMWF FORECAST VERIFICATION 12UTC

500hPa GEOPOTENTIAL

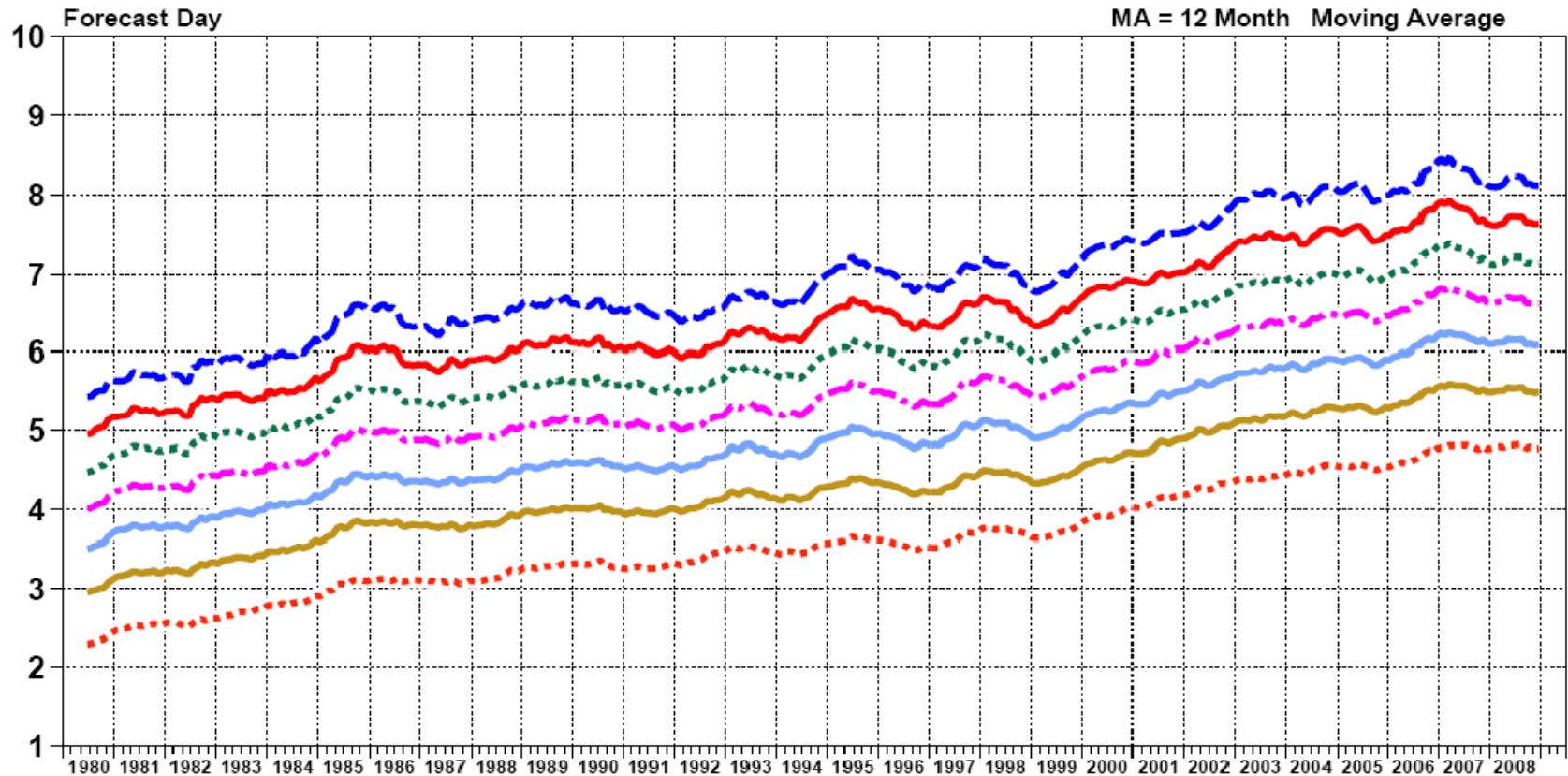
ANOMALY CORRELATION

FORECAST

N.HEM LAT 20.000 TO 90.000 LON -180.000 TO 180.000

- SCORE REACHES 60.00 MA
- SCORE REACHES 65.00 MA
- SCORE REACHES 70.00 MA
- - - SCORE REACHES 75.00 MA
- SCORE REACHES 80.00 MA
- SCORE REACHES 85.00 MA
- - - SCORE REACHES 90.00 MA

MA = 12 Month Moving Average



Understanding improvements

- The realism of the model has improved, better definition of initial condition with the introduction of 4Dvar, increasing usage of observations from remote sensing.
- In particular Mureau 1990, Simmons et. al 1995 have shown that the systematic errors (the steady drift of the model) has been reduced drastically with model improvement occurred through the 80's due for example to the introduction of the envelope orography first (Tibaldi, 1986) and then with the parametrization of sub grid effect of surface and gravity wave drag (Miller et al, 1989). ***The reduction it has been obtained in particular through improved prediction of long-waves.***

A large portion of the total variance is due to low frequency – low zonal wavenumber waves

power density of Z
500 hPa
In the NCEP
reanalysis

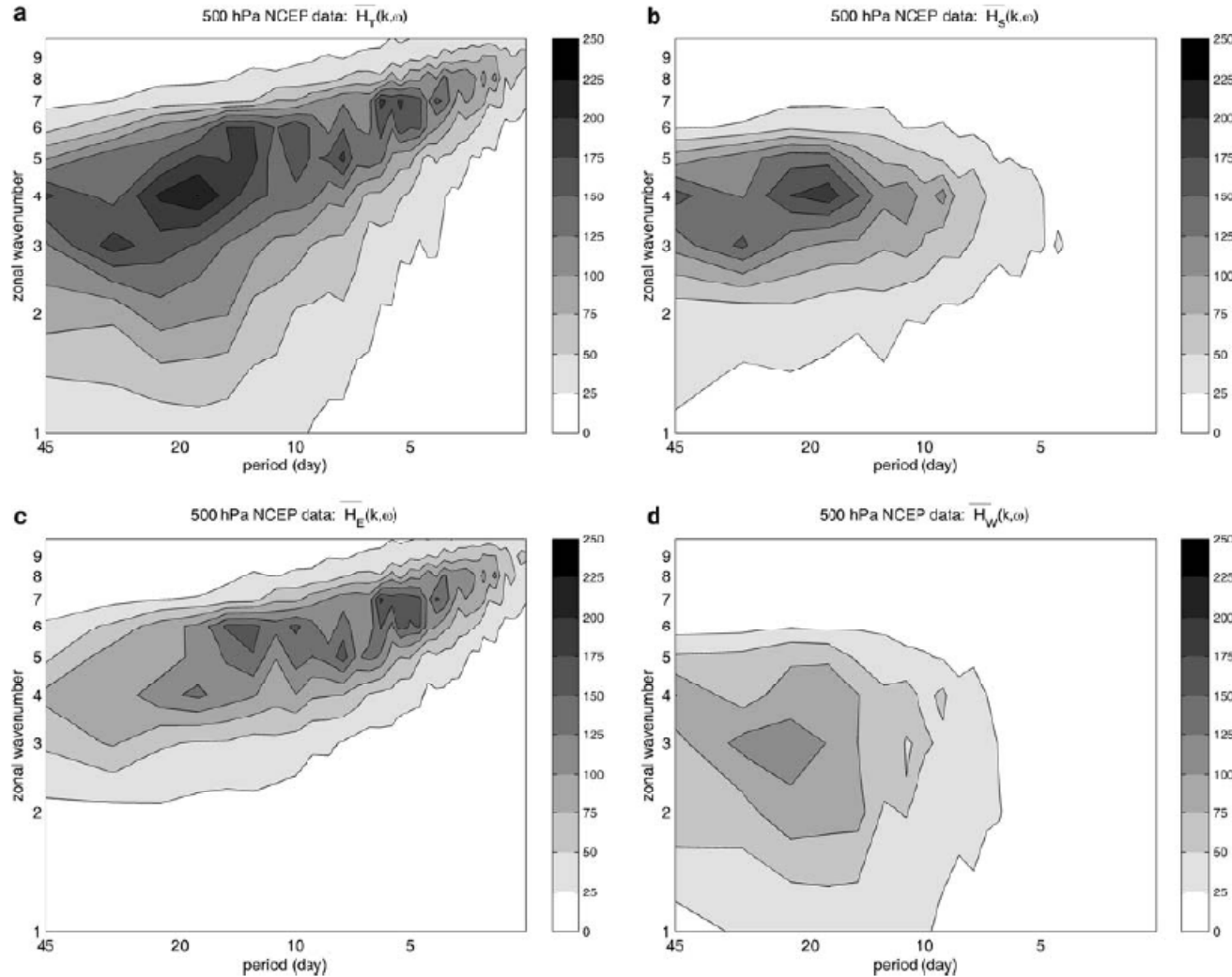


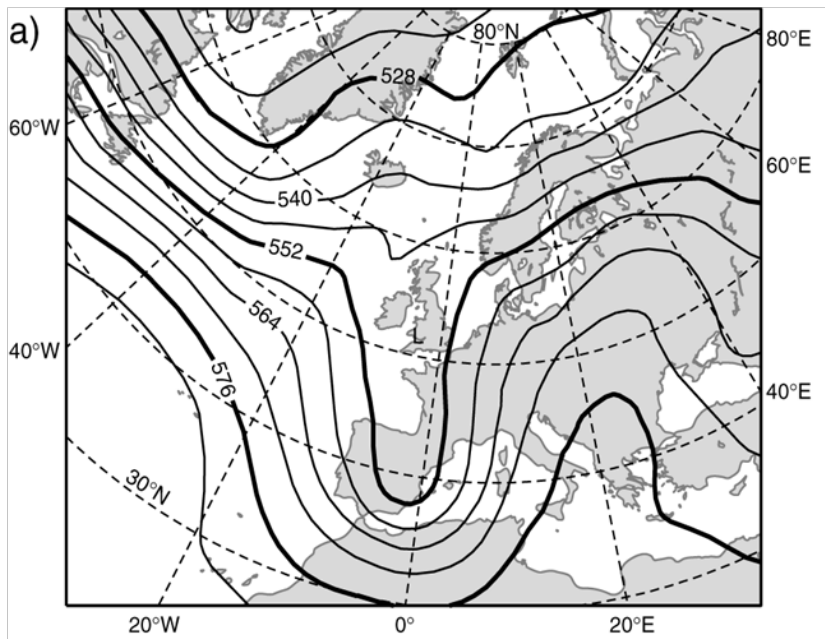
Fig. 1 Climatological average over 45 winters of Hayashi spectra for 500 hPa geopotential height (relative to the latitudinal belt 30–75°N) from NCEP data: $\overline{H_T}(k, \omega)$ (a) $\overline{H_S}(k, \omega)$ (b) $\overline{H_E}(k, \omega)$ (c) $\overline{H_W}(k, \omega)$ (d). The Hayashi spectra have been obtained multiplying the spectra by $k \cdot \omega / 2\pi$. The units are $m^2/s \times 10^{-5}$

How refinements in the forecasting system have projected on to the prediction a particular synoptic pattern ?

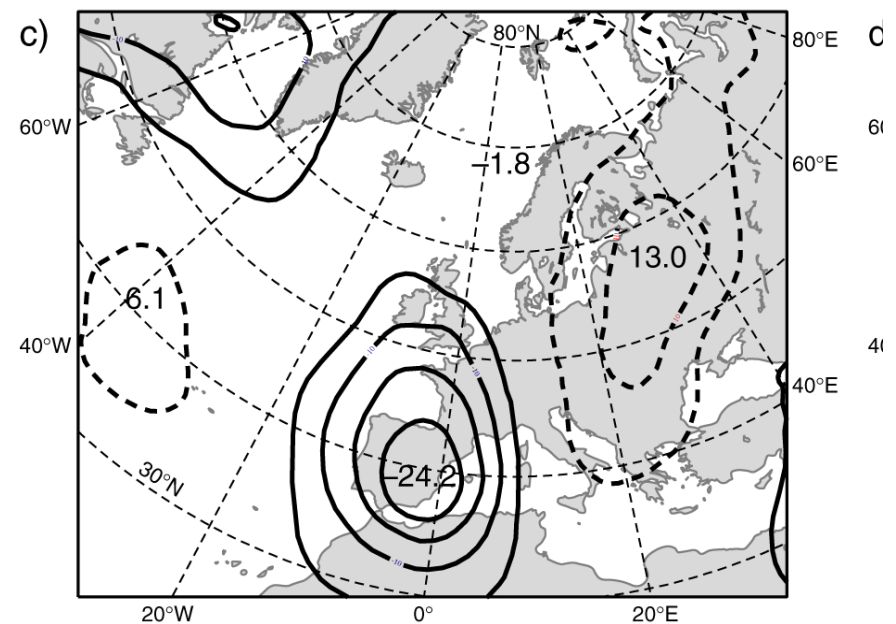
Strong southerly flow condition (SSF), a pattern associated with heavy rain on the southern side of the Alps

Grazzini, 2007

SSF Z500 reference pattern

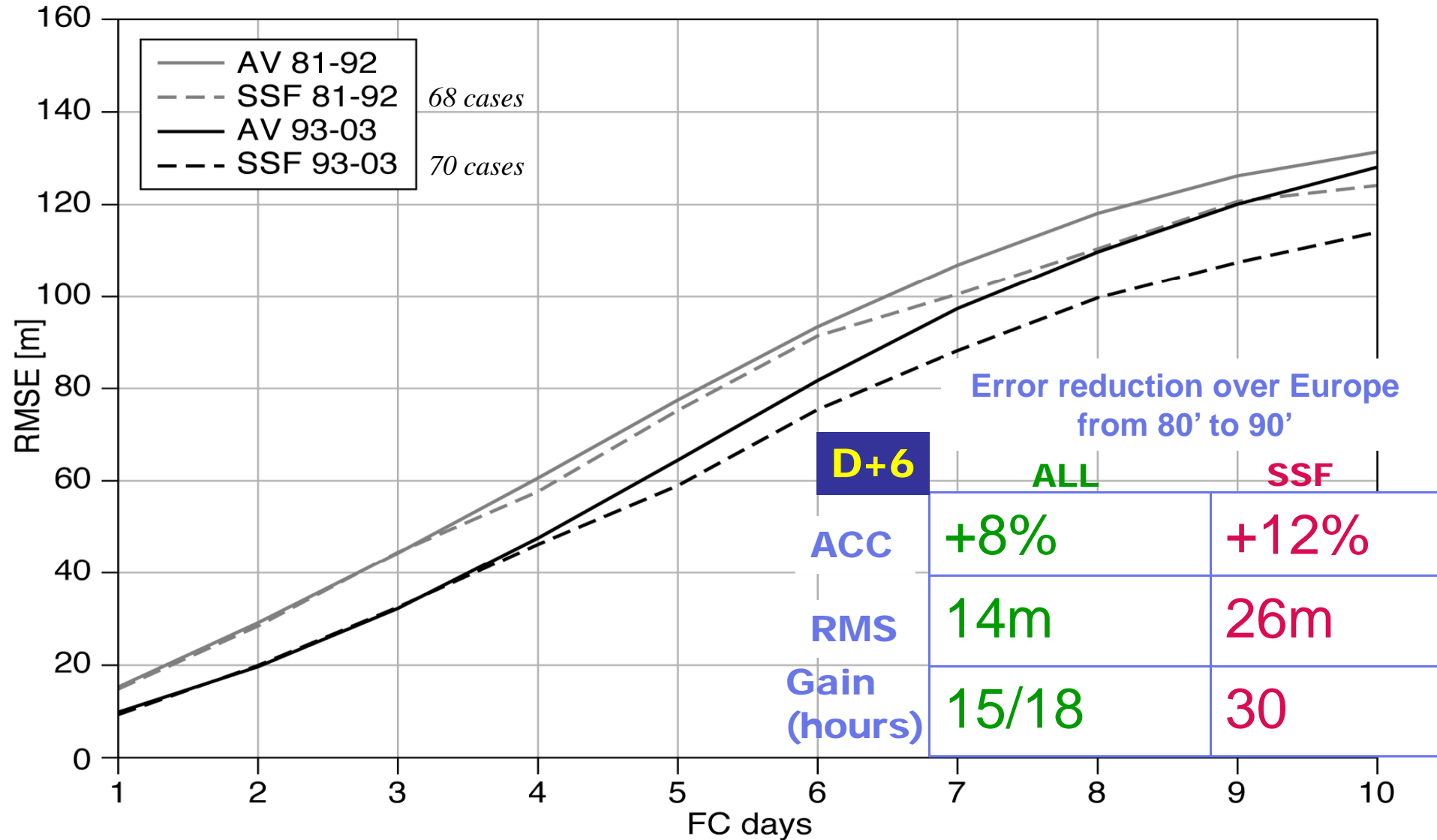


SSF Z500 reference anomaly

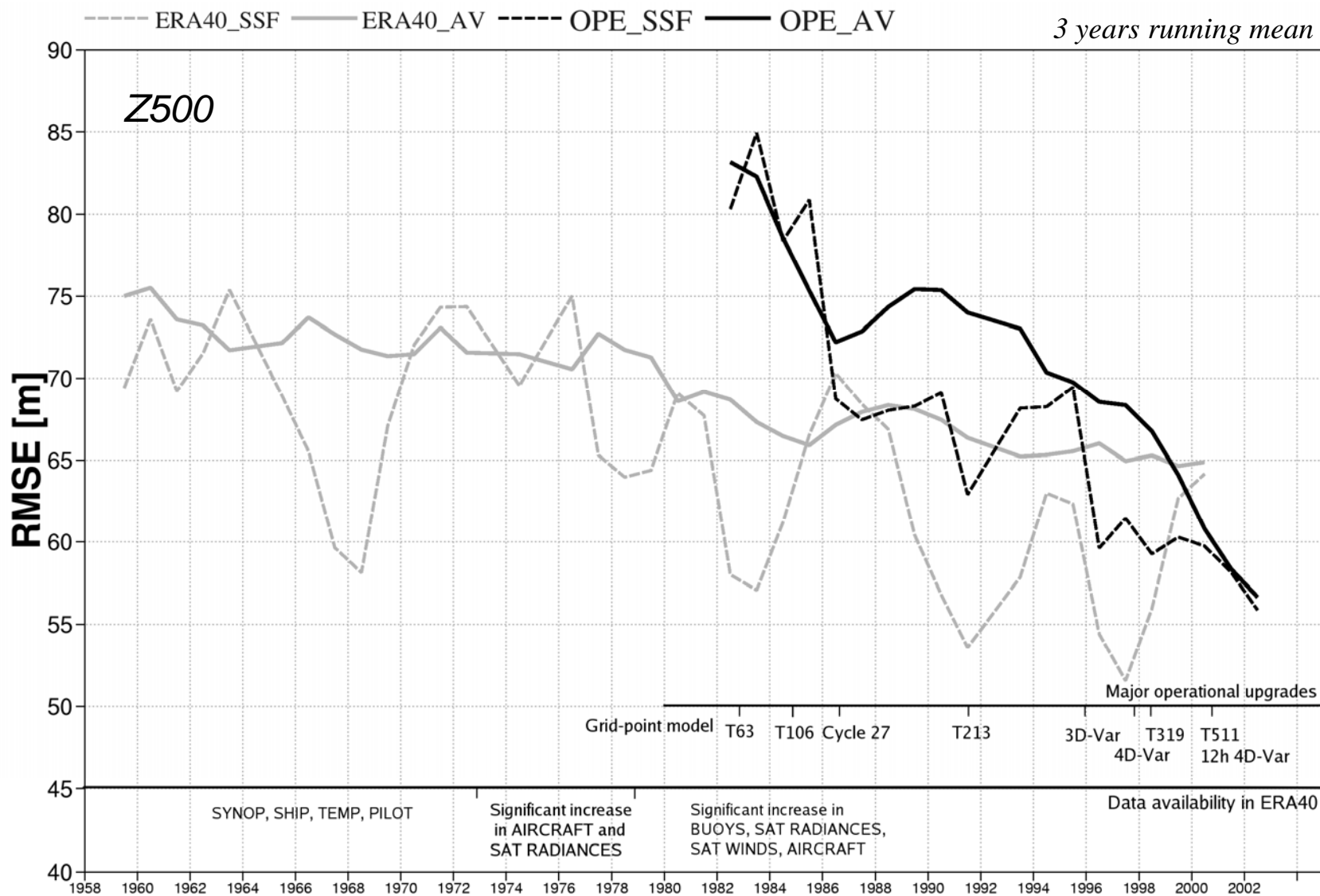


(for the definition of and identification of the reference pattern see also Martius et al., 2006)

RMSE Z500 over Europe in Spring and Autumn days only



Trend of (D+4/D+6) RMSE over Europe in Spring+Autumn

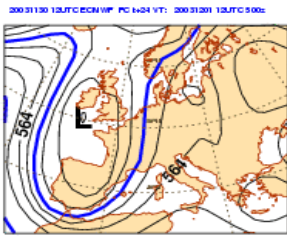


Grazzini, 2007

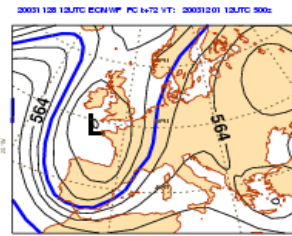
Is this pattern potentially more
predictable ?

An example of SSF predictability: 1 December 2003

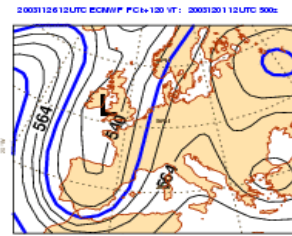
OP D+1



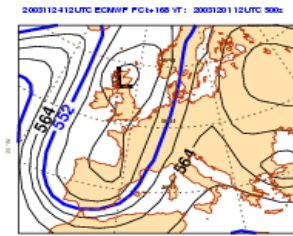
OP D+3



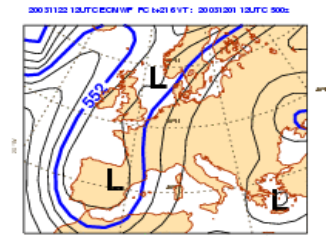
OP D+5



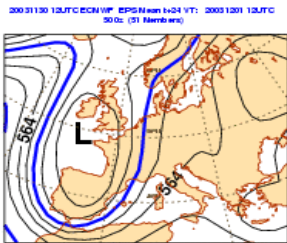
OP D+7



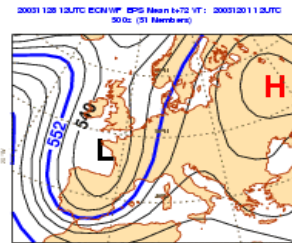
OP D+9



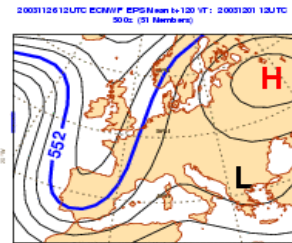
EM D+1



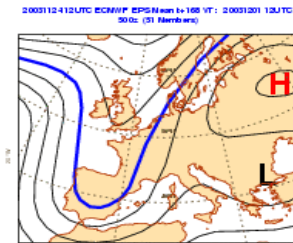
EM D+3



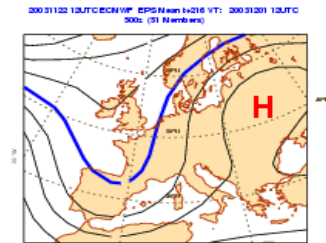
EM D+5



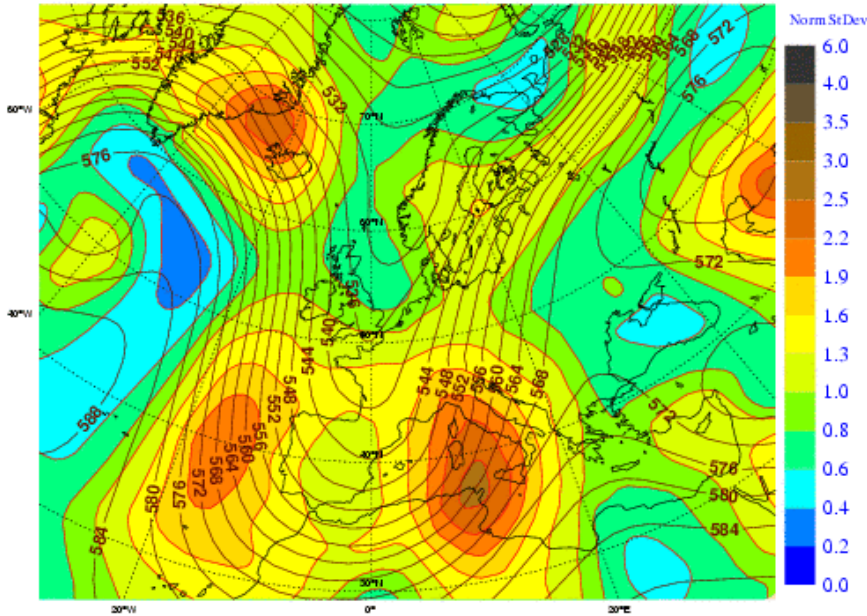
EM D+7



EM D+9



Friday 24 October 2008 12UTC ECMWF Forecast 1+120 VT: Wednesday 29 October 2008 12UTC
500hPa Geopotential Ensemble Mean and Normalised Standard Deviation (shaded)

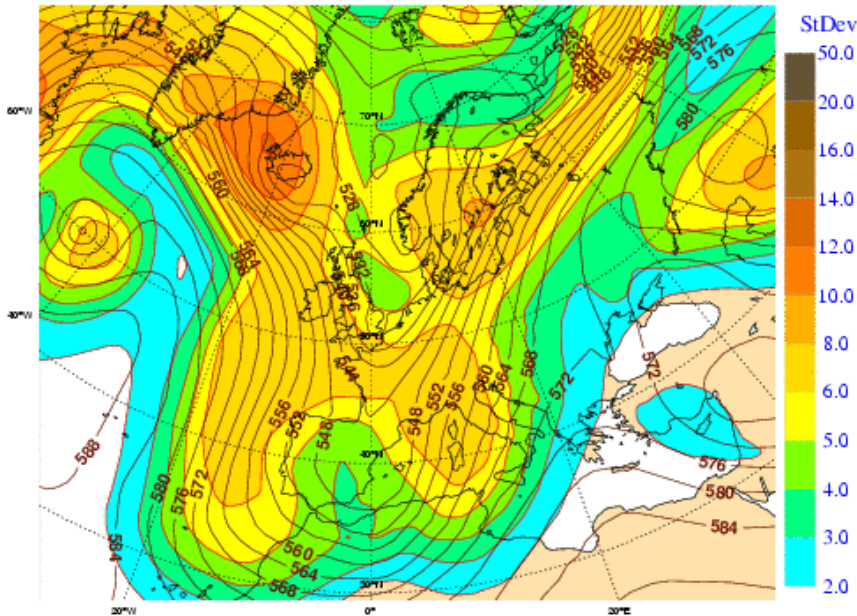


A different SSF case:
EPS spread
distribution.

Normalised spread

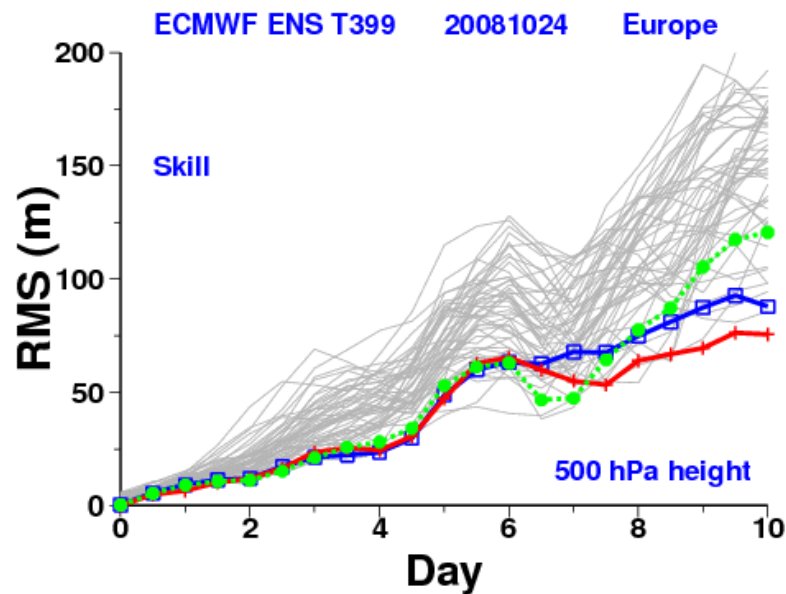
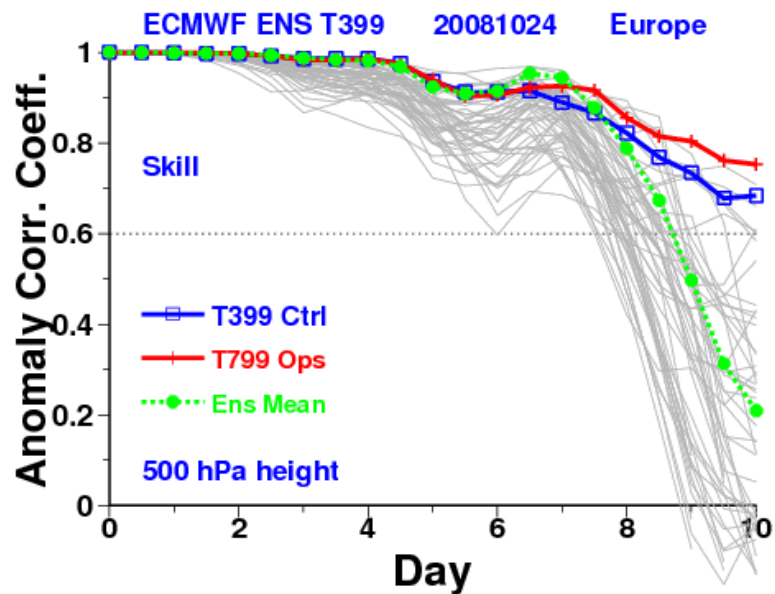
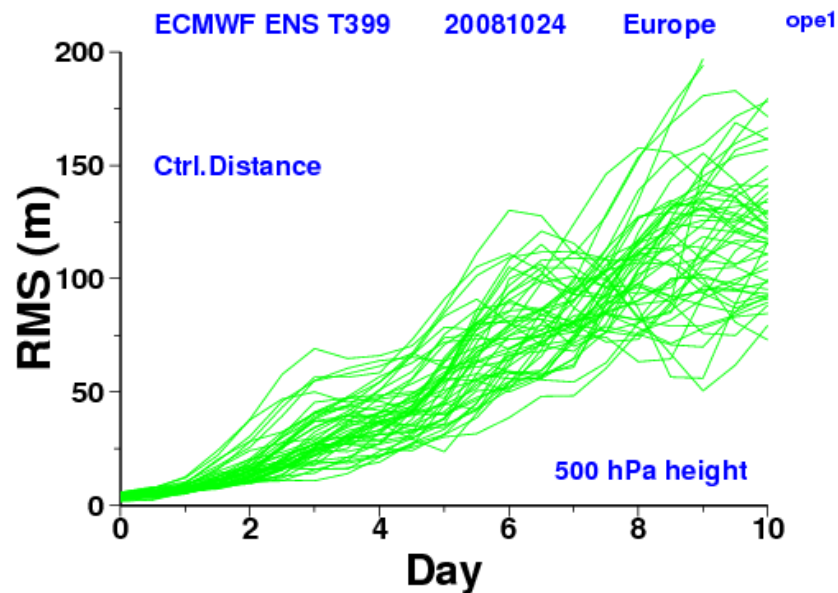
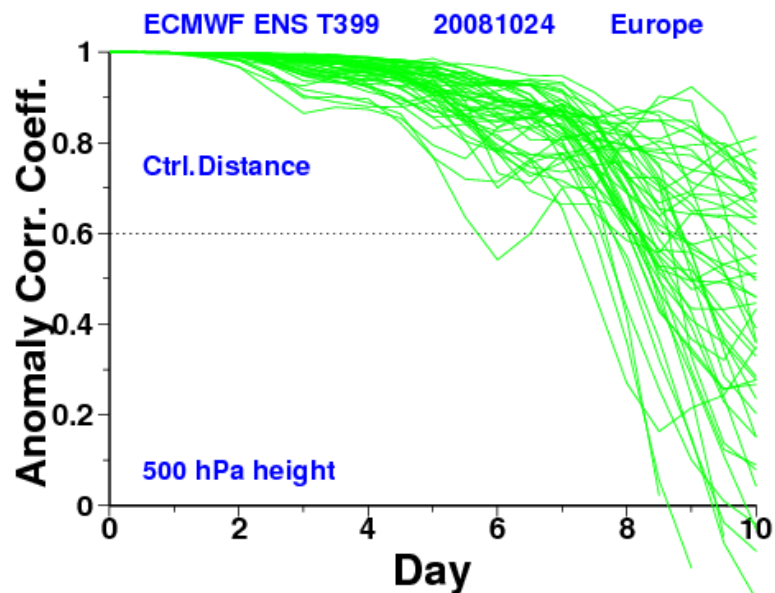
In the normalised spread it
is evident a wave
pattern associated with a
minimum on the ridges

Friday 24 October 2008 12UTC ECMWF Forecast 1+120 VT: Wednesday 29 October 2008 12UTC
500hPa Geopotential Deterministic Forecast and Standard Deviation (shaded)



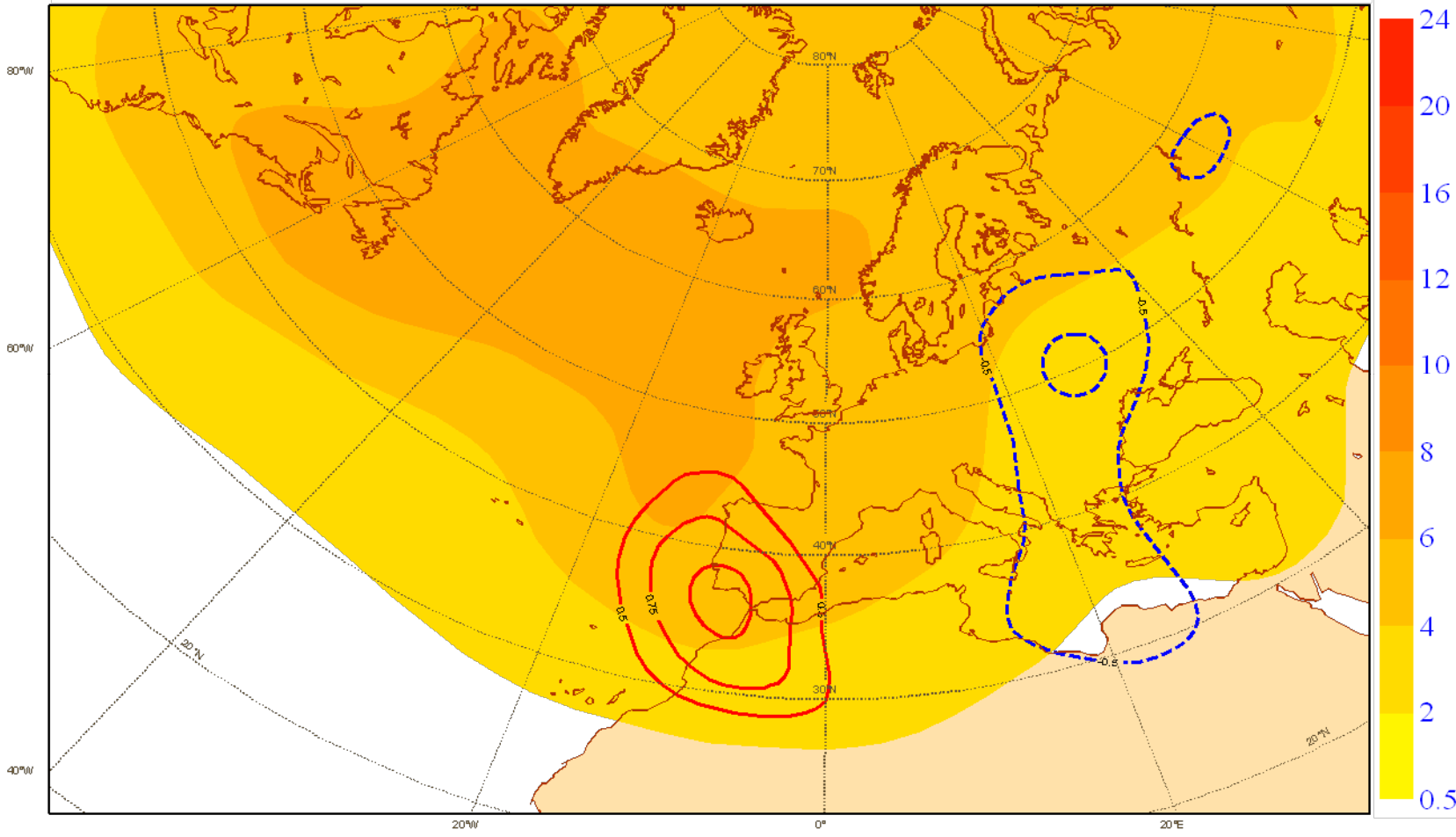
Spread

The same case : EPS performance compared with deterministic models



Mean predictability of Z 500 estimated by EPS member spread

Mean EPS D+5 member std 500hPa Z FC during 69 SSF cases (1995-2003)
red/blue count are standardized anomalies from 10 days lagged dataset (proxi for average conditions)



Evidences of Predictability increase also at smaller scales sensitivity to the growth of internal domain perturbations

SSF flow type

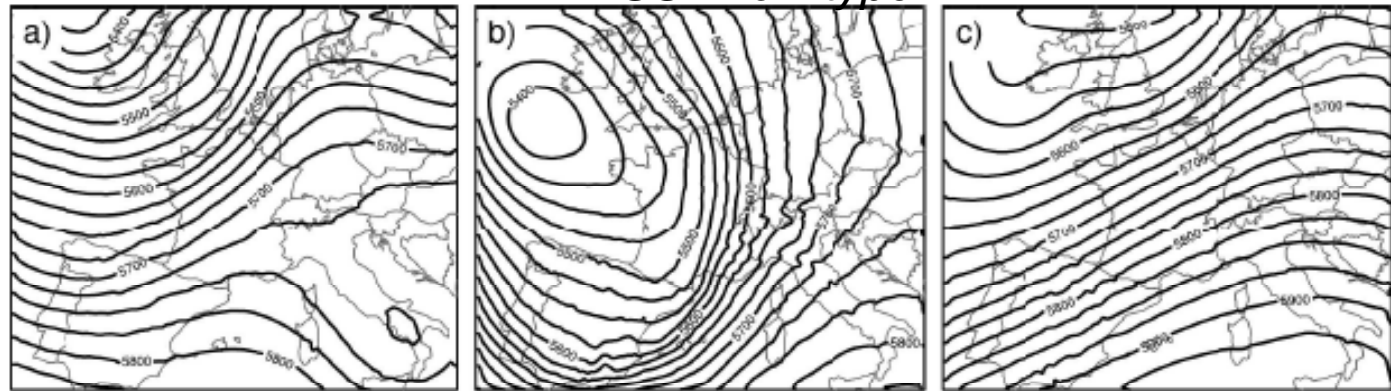
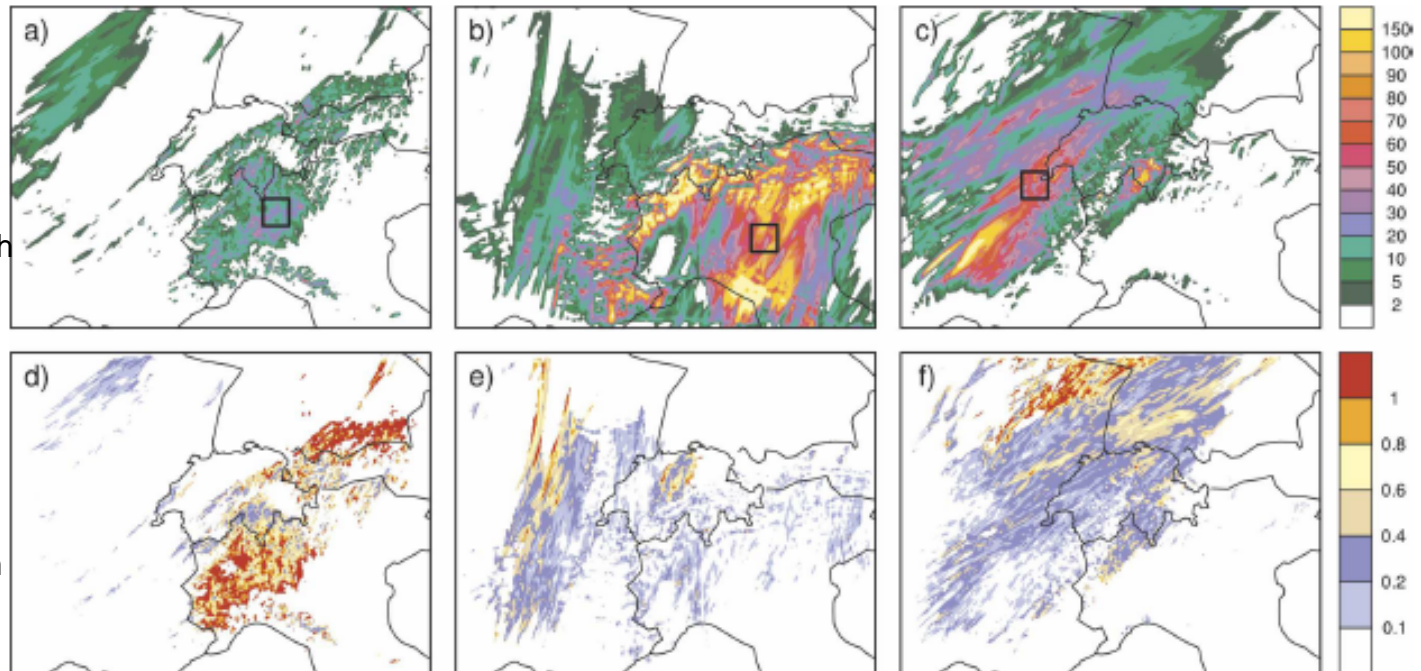


FIG. 2. The 500-hPa geopotential height (m) valid at 0000 UTC on (a) 17 (IOP2a), (b) 20 (IOP2b), and (c) 25 (IOP3) Sep 1999. The data are from the 7-km LM simulation driven by the ECMWF analysis.

Greater loss of predictability occurs over moist convectively unstable regions that are able to propagate energy against the mean flow (absolute instability). From linear analysis of absolute instability theory we see that for $U > U_{crit} = Nm^2 / (m^2 + k^2) \cdot \sqrt{m^2 + k^2}$ upstream propagation of gravity waves is inhibited, growing perturbation are swept away by lateral boundary condition, increase of predictability.



Ens mean of 30h accumulated precip

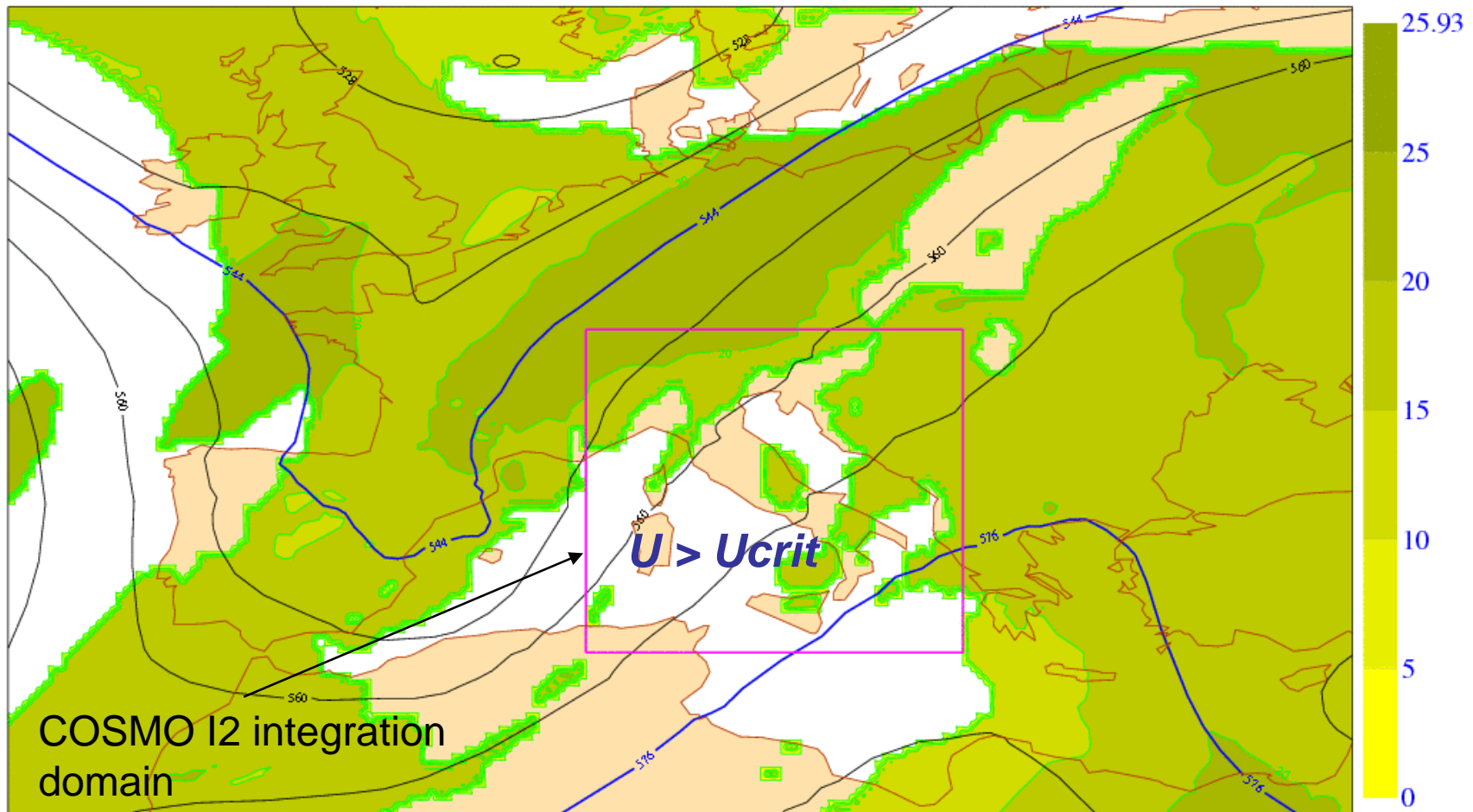
Spread of 30h accumulated precip

Hohenegger et al. 2006

An attempt to objectively estimate predictability of precip.

Using the technique described in Hohenegger et al. 2006, absolute stability have been estimated . The white area it is showing regions where predictability should not be degraded by the presence upstream growth and propagation of gravity waves.

Wind velocity U 500 hPa 29/10/2008 12UTC – White areas $U > U_{crit}$



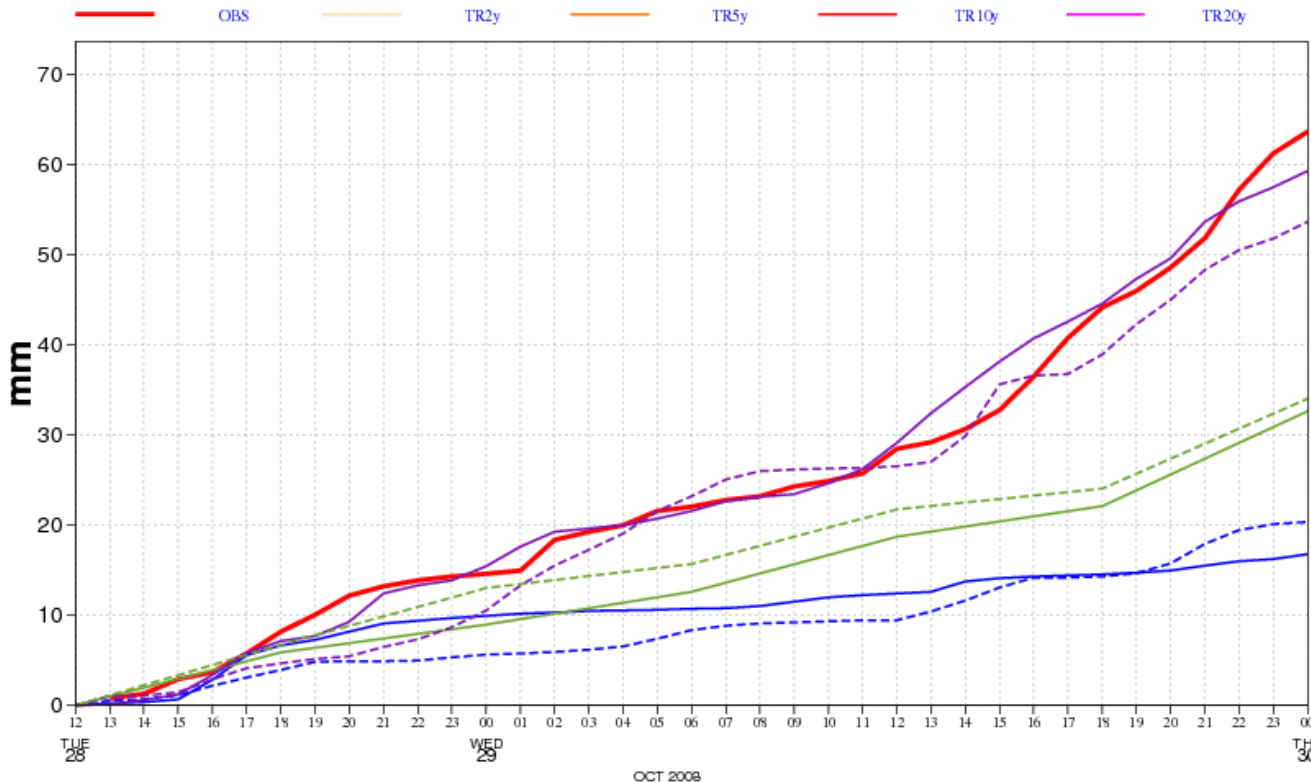
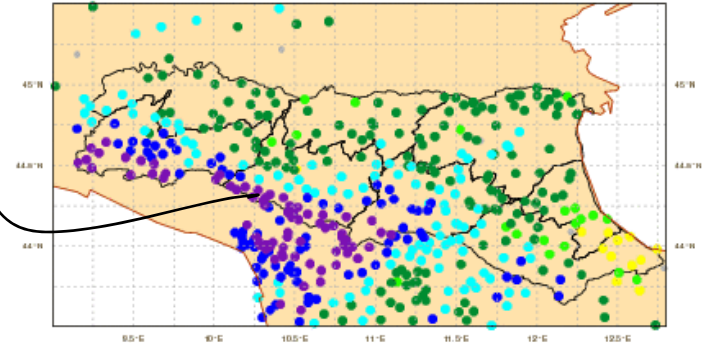
Remarkable short-term consistency among successive runs

Averaged precip over warning area E (3000Km2)

PRECIPITAZIONE OSSERVATA E PREVISTA SULLA MACRO AREA - E -
 osservazioni e tempi di ritorno (TR) riferiti a 24h
 I2 : 410 grid-points, I7 : 67grid-points, OBS: 45

OBS: 20081028 12 - 20081030

• 0 - 2 • 2 - 5 • 5 - 10 • 10 - 25 • 25 - 50 • 50 - 100 • 100 - 200



Solid 00 UTC runs
 Dash 12 UTC runs

COSMO I7: 2008102812
 I2: 2008102812
 ECMWF: 2008102812

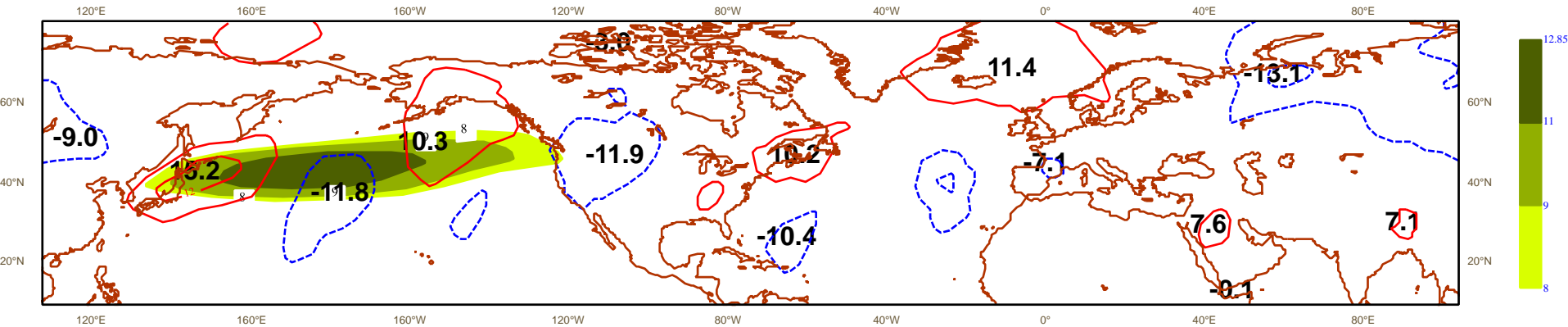
So far....

- We have shown evidences of higher predictability for this flow type.
- Why ? Can we learn something on atmospheric predictability ?
- An interesting feature to note is that SSF are triggered by wave breaking at the end of a Rossby wave packet travelling from upstream regions

Propagation of wave packets leading to SSF conditions

Lag composite of 250 hPa v-component and envelope*
SSF cases between 1980-2001 (ERA40)
Autumn: 45 cases

D-6

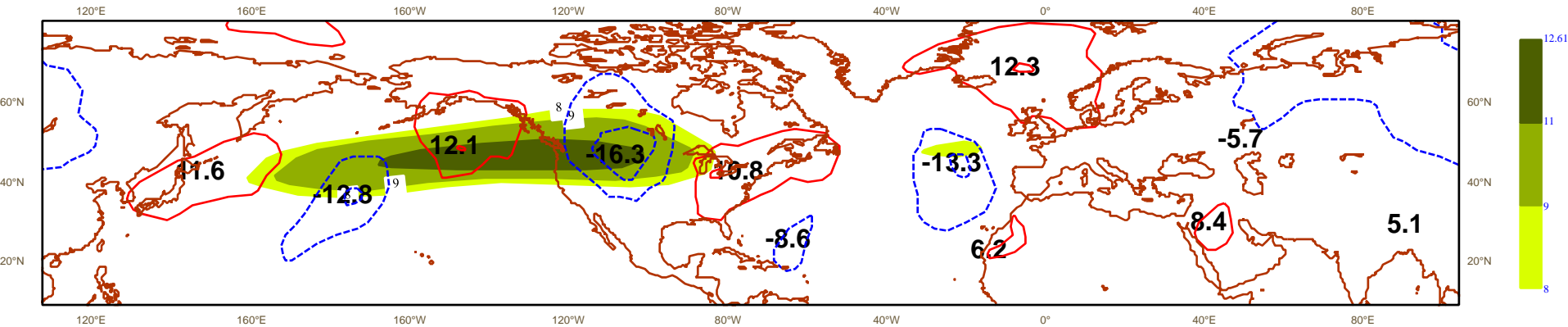


*As defined in Zimin, Szunyogh et. al., Mon. Wea. Rev, May 2003

Propagation of wave packets leading to SSF conditions

Lag composite of 250 hPa v-component and envelope*
SSF cases between 1980-2001 (ERA40)
Autumn: 45 cases

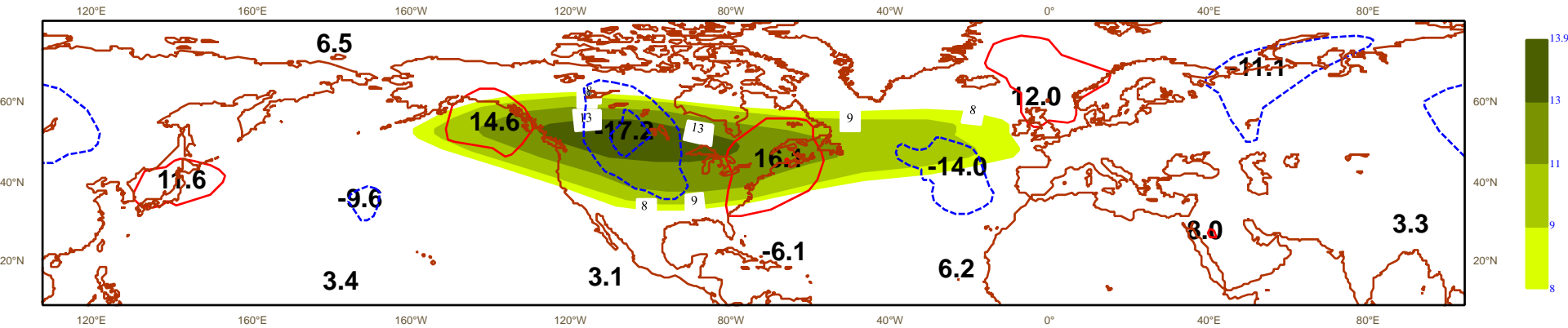
D-5



Propagation of wave packets leading to SSF conditions

Lag composite of 250 hPa v-component and envelope*
SSF cases between 1980-2001 (ERA40)
Autumn: 45 cases

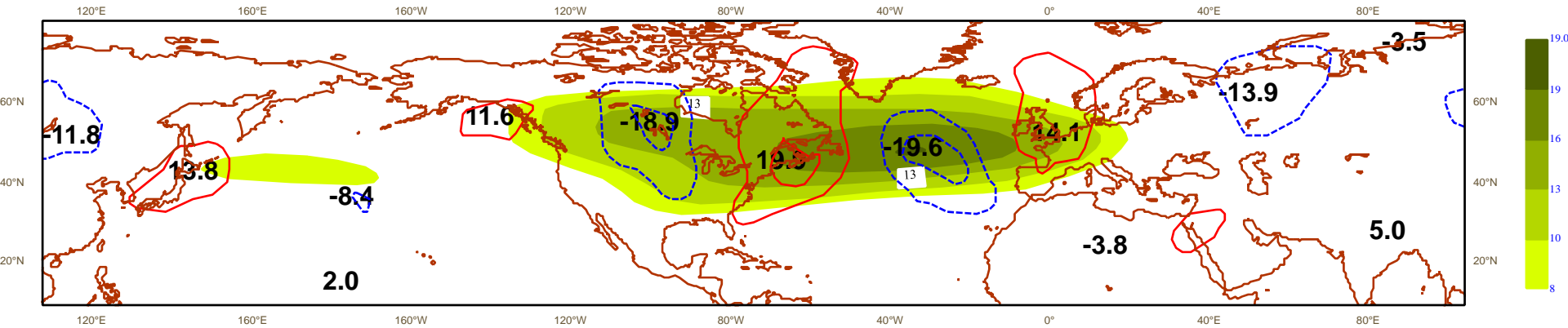
D-4



Propagation of wave packets leading to SSF conditions

Lag composite of 250 hPa v-component and envelope*
SSF cases between 1980-2001 (ERA40)
Autumn: 45 cases

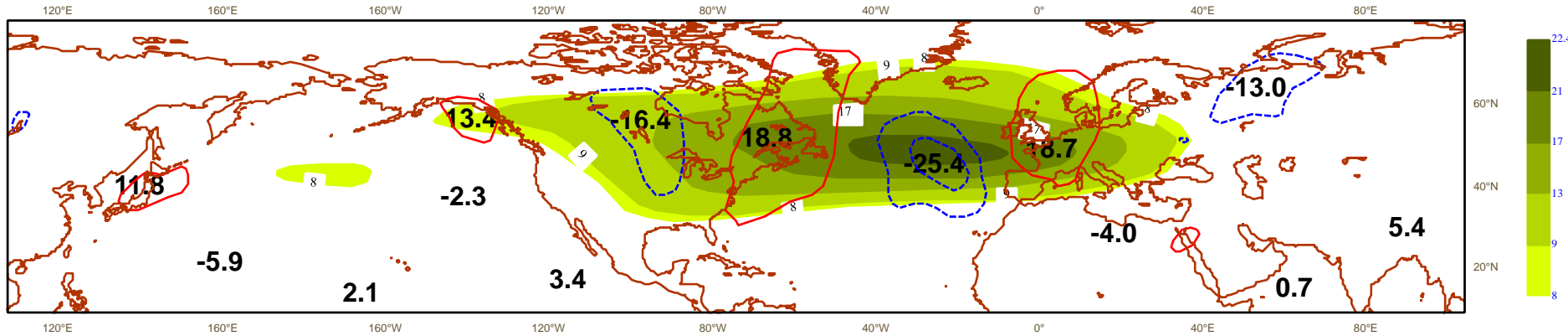
D-3



Propagation of wave packets leading to SSF conditions

Lag composite of 250 hPa v-component and envelope*
SSF cases between 1980-2001 (ERA40)
Autumn: 45 cases

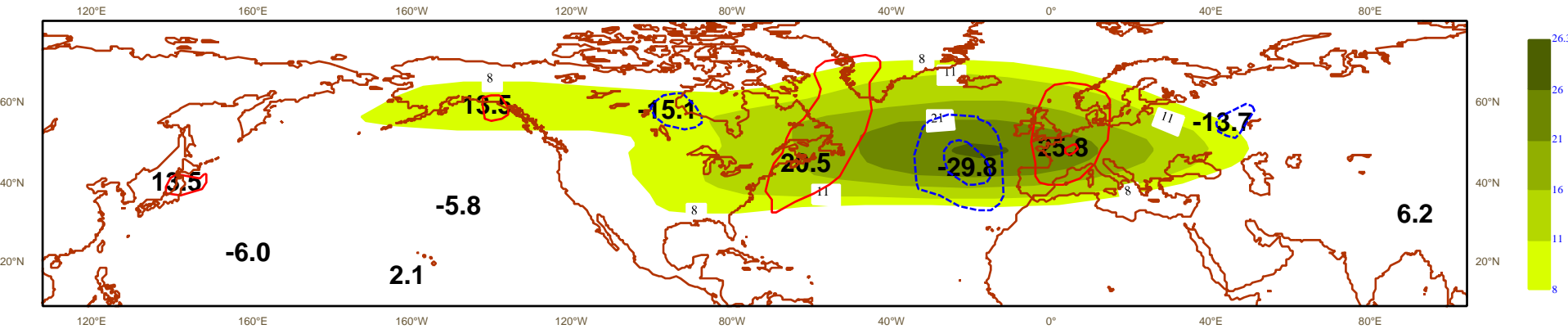
D-2



Propagation of wave packets leading to SSF conditions

Lag composite of 250 hPa v-component and envelope*
SSF cases between 1980-2001 (ERA40)
Autumn: 45 cases

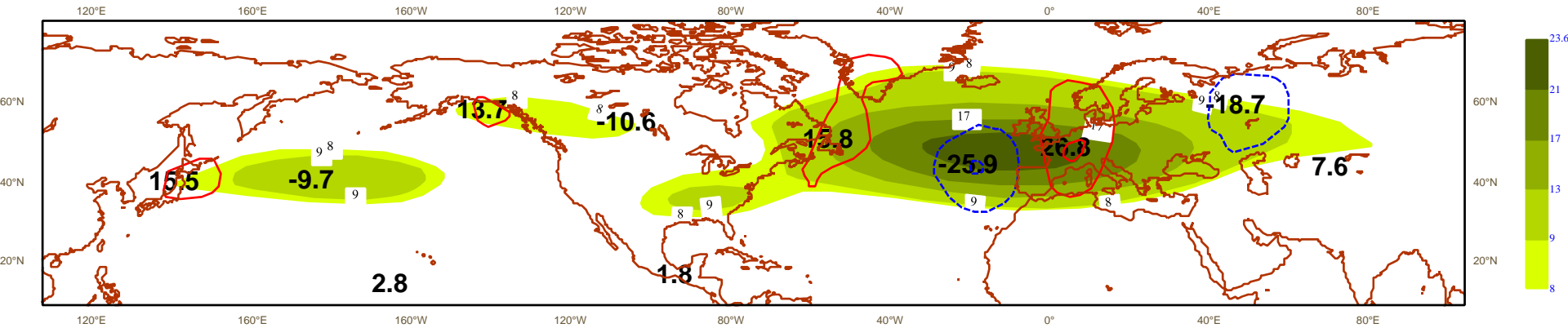
D-1



Propagation of wave packets leading to SSF conditions

Lag composite of 250 hPa v-component and envelope*
SSF cases between 1980-2001 (ERA40)
Autumn: 45 cases

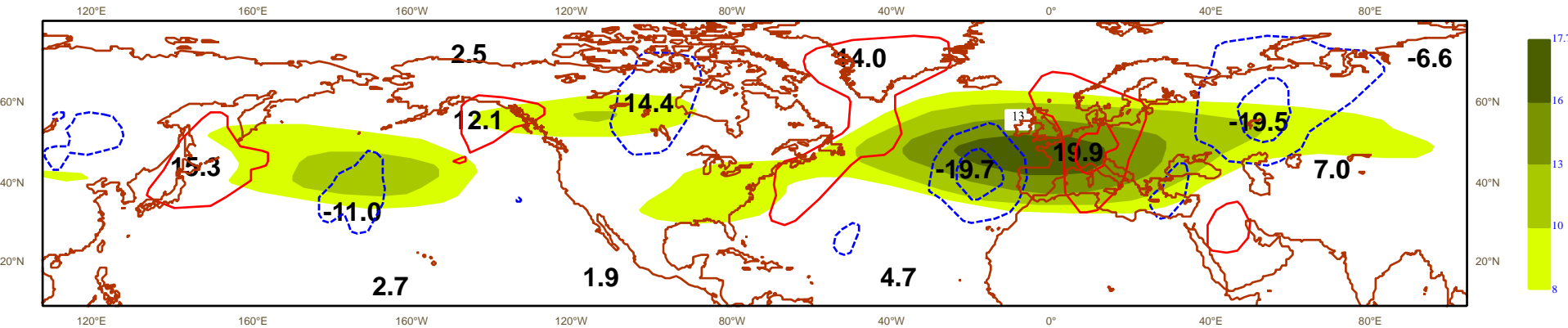
DO



Propagation of wave packets leading to SSF conditions

Lag composite of 250 hPa v-component and envelope*
SSF cases between 1980-2001 (ERA40)
Autumn: 45 cases

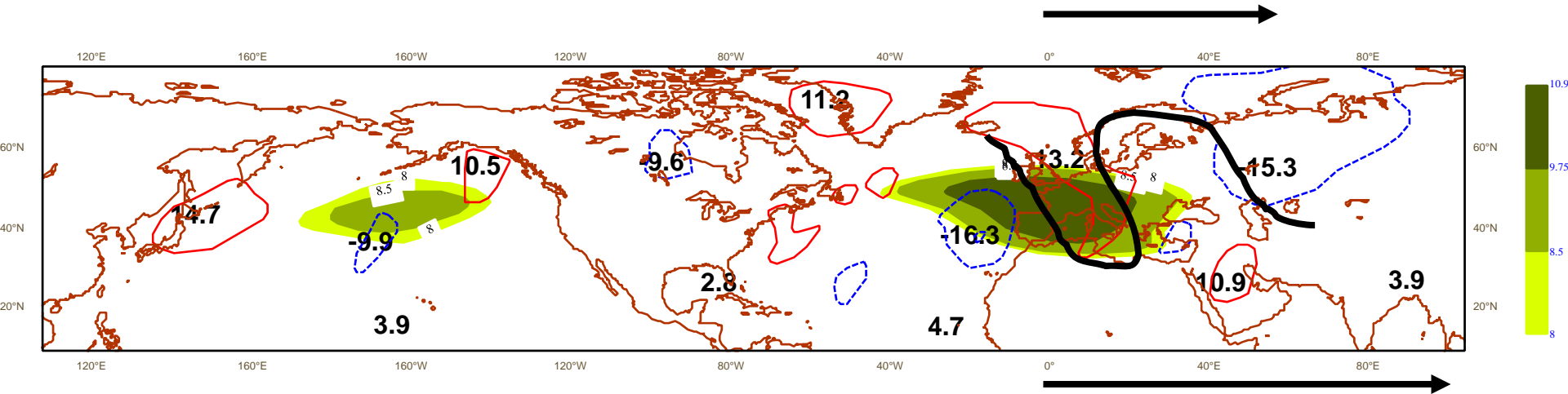
D+1



Propagation of wave packets leading to SSF conditions

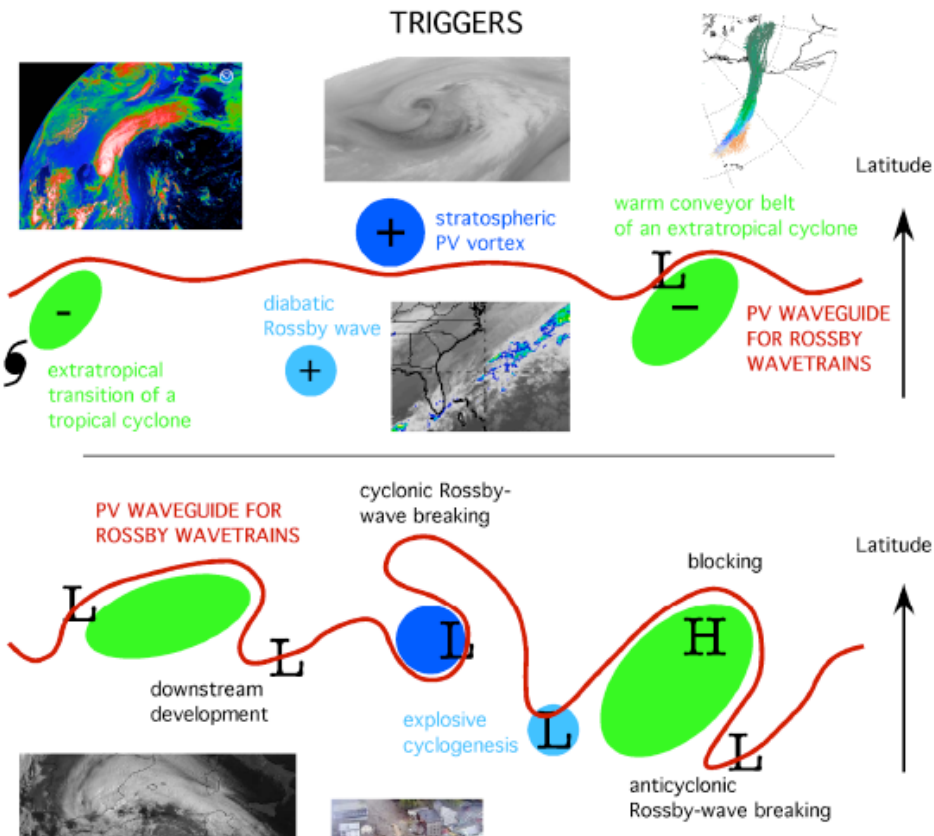
Lag composite of 250 hPa v-component and envelope*
SSF cases between 1980-2001 (ERA40)
Autumn: 45 cases

D+2



Cyclonic wave breaking (Martius 2007)

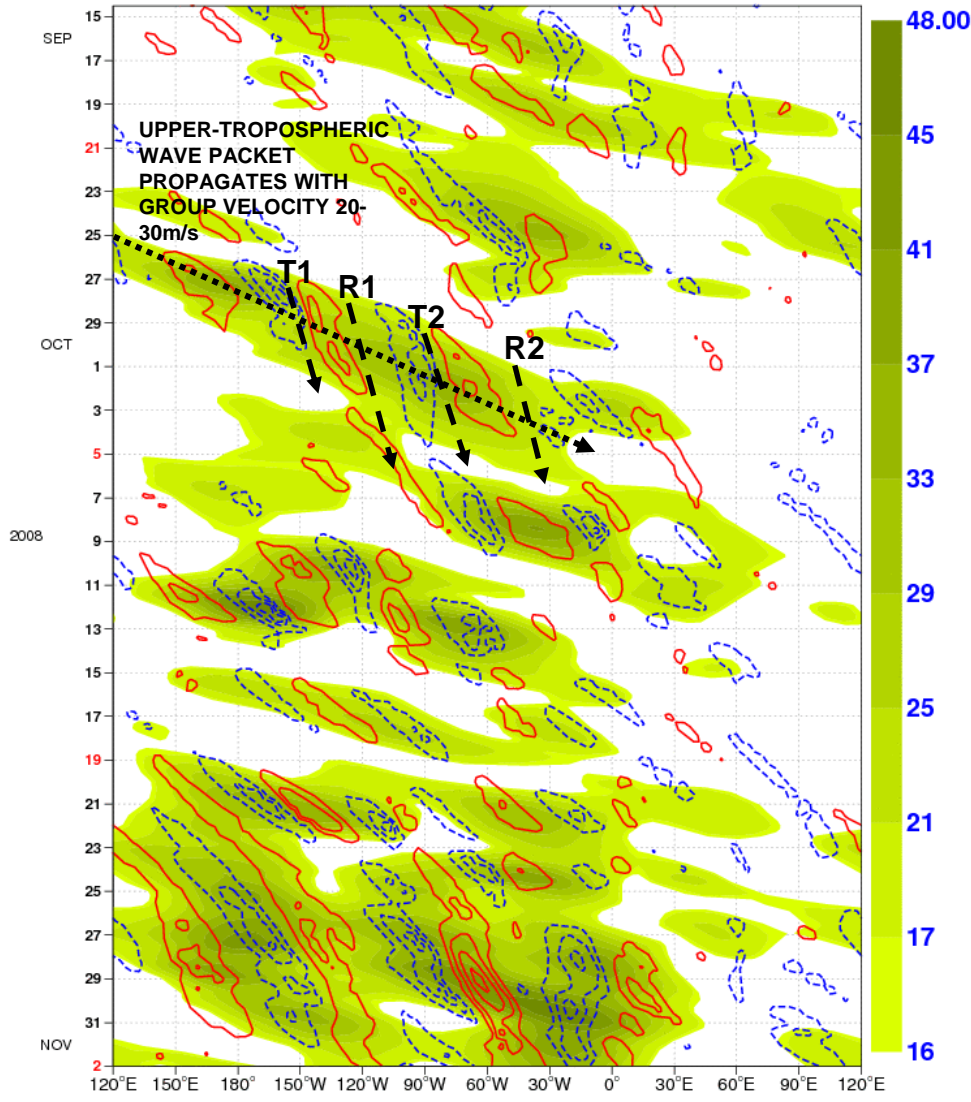
RWP and synoptic activity



Szunyogh et al.2008, BAMS

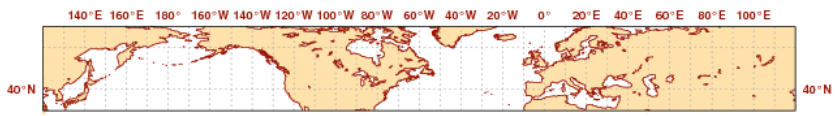
Thorpe Science Plan: “*The skilful prediction of Rossby wave-train activity is often a requisite for forecasting the synoptic-scale setting within which smaller-scale, high-impact weather events evolve at forecast time ranges out to two weeks.* Rossby wave trains are initiated by components of the flow, such as: i) downstream baroclinic development; ii) the interaction of extratropical flows with large-scale topography; iii) variations in moist tropical convective-heating associated with ENSO, MJO, and higher-frequency convective variability within the tropical oceanic convergence zones and monsoon regions. Other aspects of interest are: i) the establishment and maintenance of Rossby wave guides; ii) triggering of sub-synoptic scale features by individual synoptic waves within wave trains and their feed back into the dispersion of the wave train” (Shapiro and Thorpe 2004).

Hovmoeller diagram of 250-hPa meridional wind component and envelope (zonal wavenumbers 3-9)

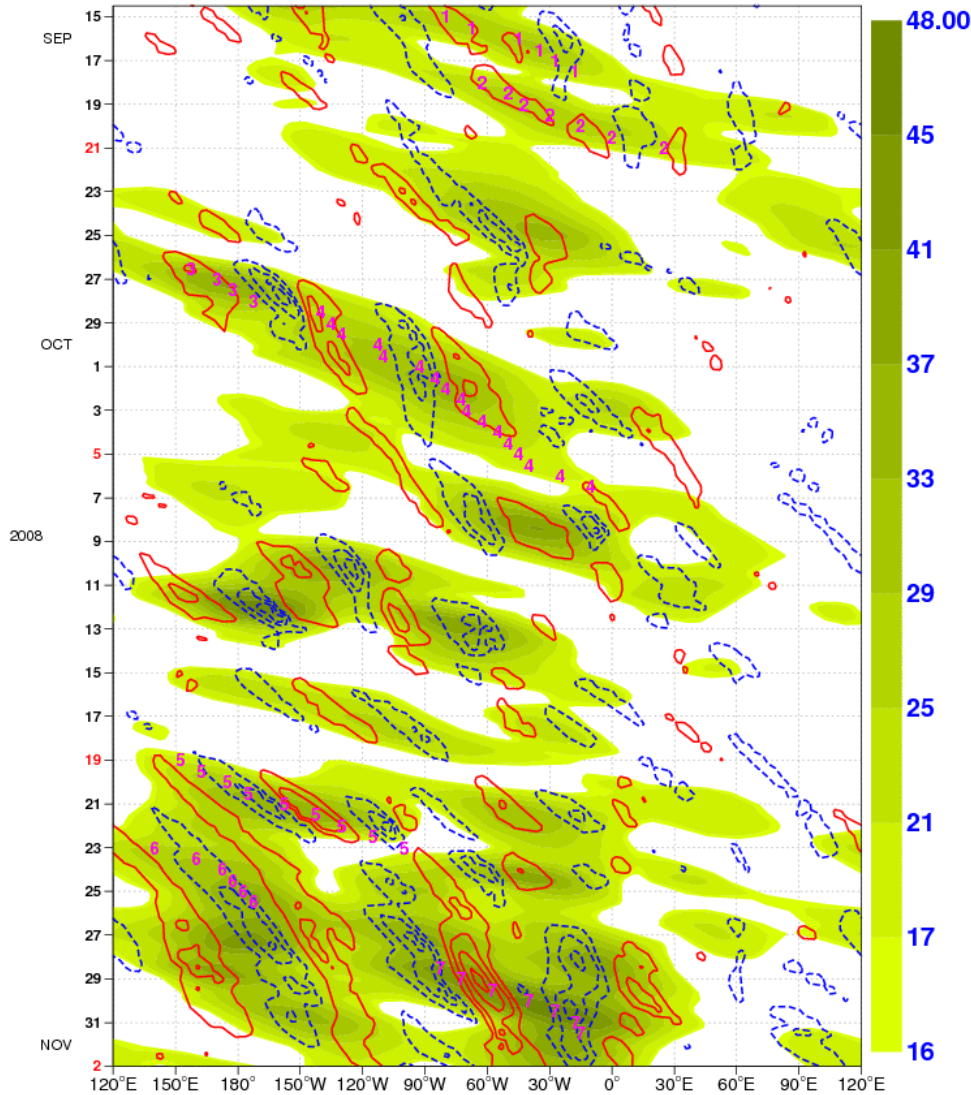


Does RWP activity influence predictability ?

SYNOPTIC-SCALE TROUGH (T) AND RIDGE (R) FEATURES PROPAGATE WITH PHASE VELOCITY OF 5-10 m s⁻¹



Hovmoeller of v-vel 250 Expver 0001 (65.0N-35.0N) envelope spectral band 3-9



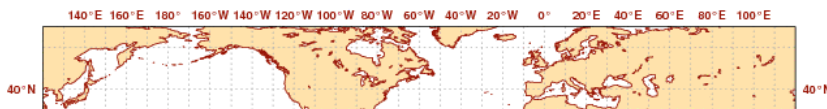
Wave packet tracking algorithm

DATA: 12h interval wind V-component at 250 hPa taken from the ECMWF ERA40 reanalysis in the period 1958-2001 and from ECMWF operational analyses for the period 2002-2008. Data are interpolated at $2.5^\circ \times 2.5^\circ$ degree resolution.

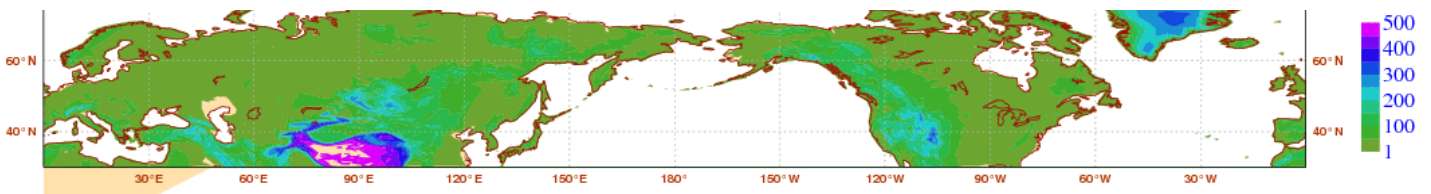
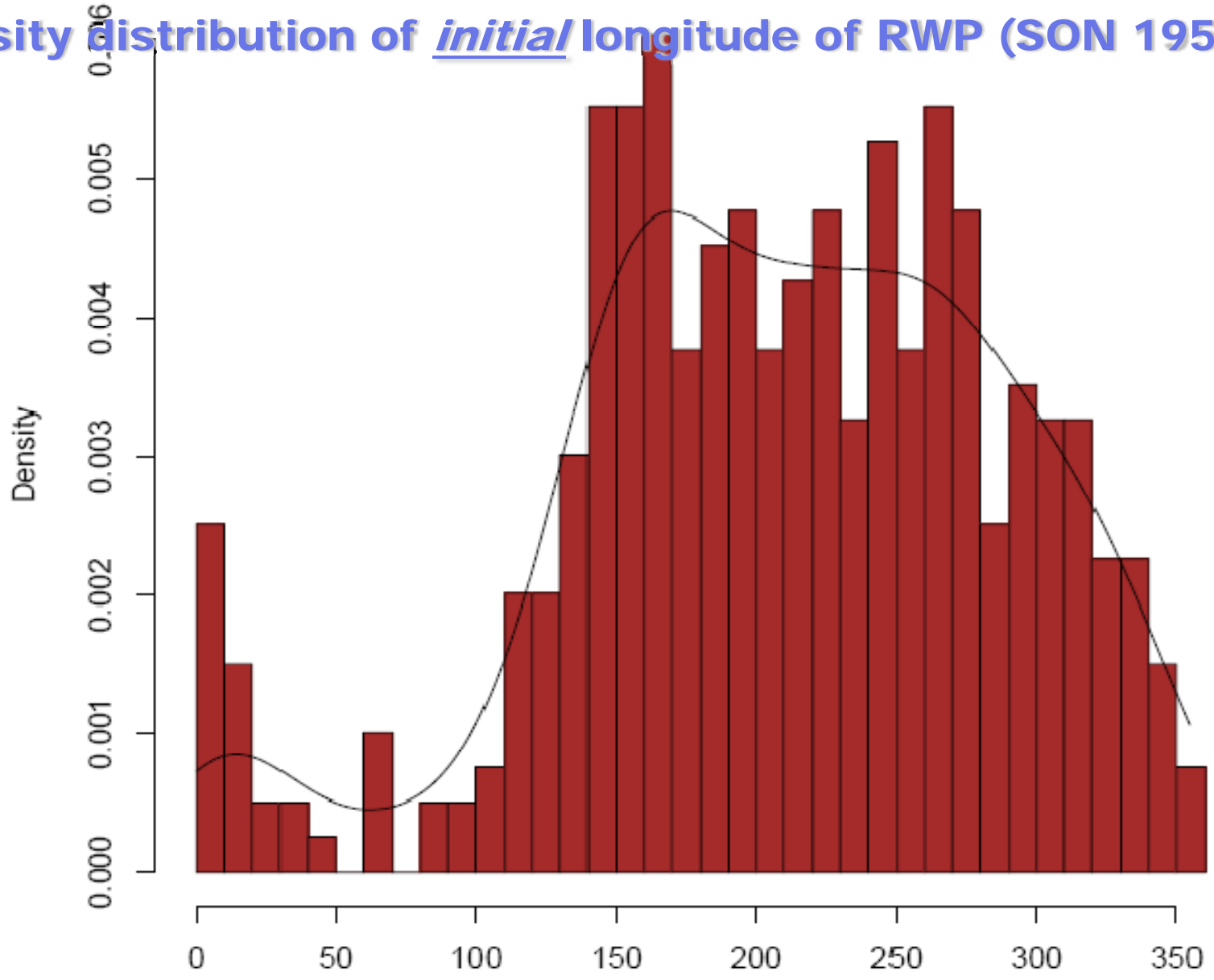
Main steps of planetary tracking procedure:

- 1) Computation of planetary waves envelope over NH based on a Hilbert transform technique described in (Zimin et al. 2003)
- 2) Latitudinal average of the envelope over the belt **35-65N**
- 3) Tracking of the envelope maxima: we assume that temporally subsequent maxima belongs to the same packet if group velocity remain within a physical range appropriate for that wave number interval and the amplitude of the envelope is above a certain threshold based on daily standard deviation of the envelope. Multiple packet are allowed.

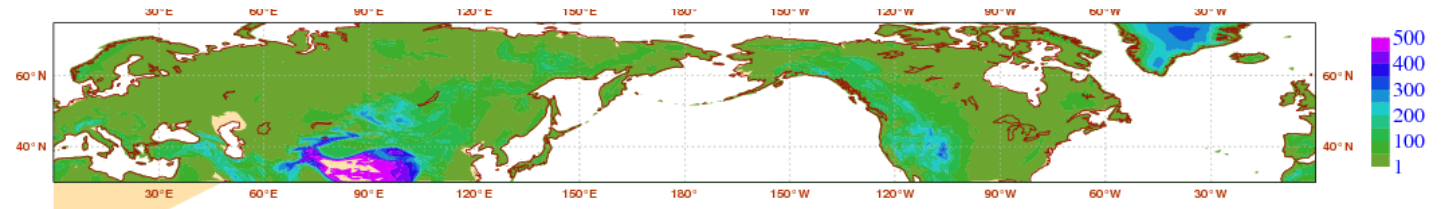
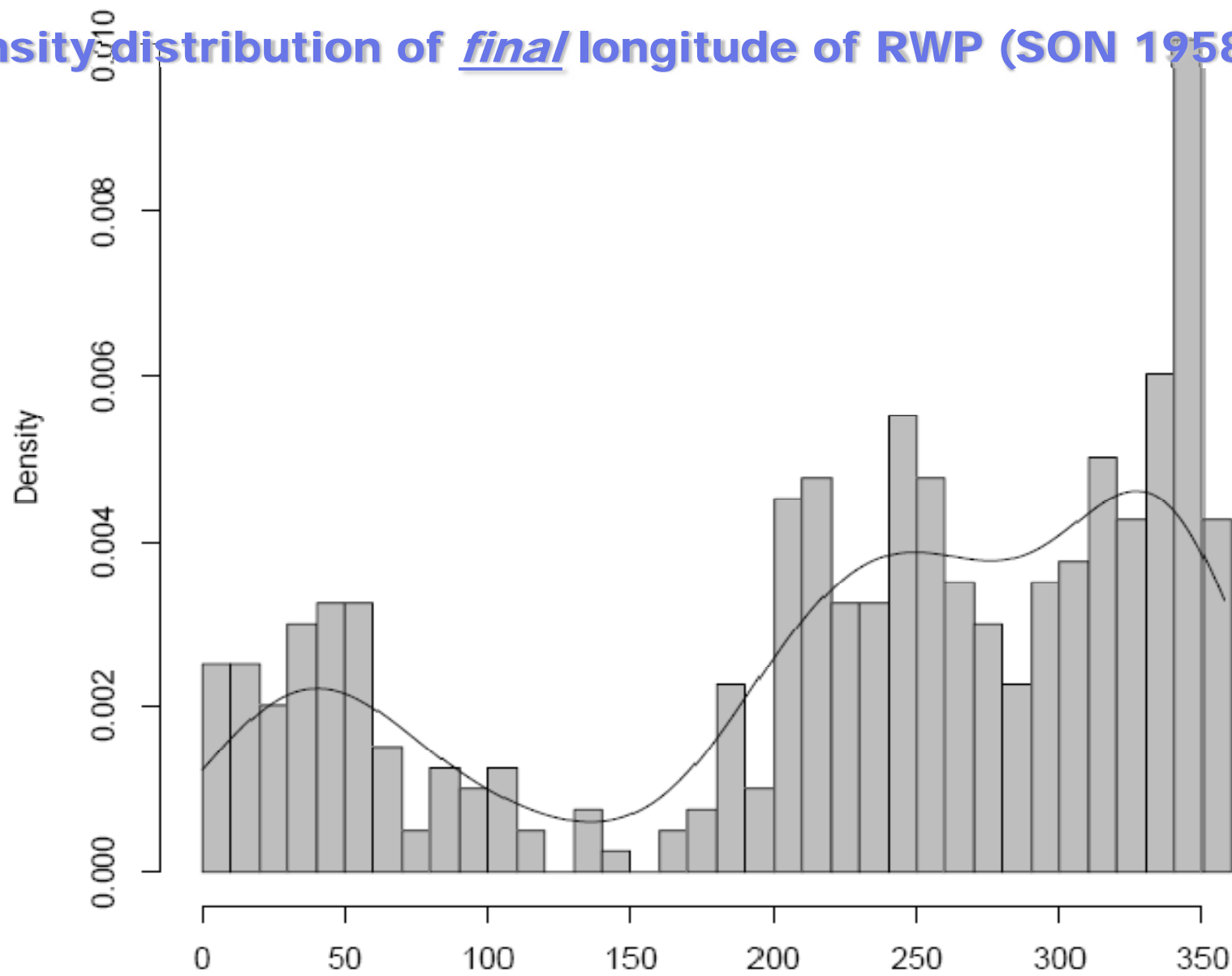
Grazzini & Lucarini, 2009



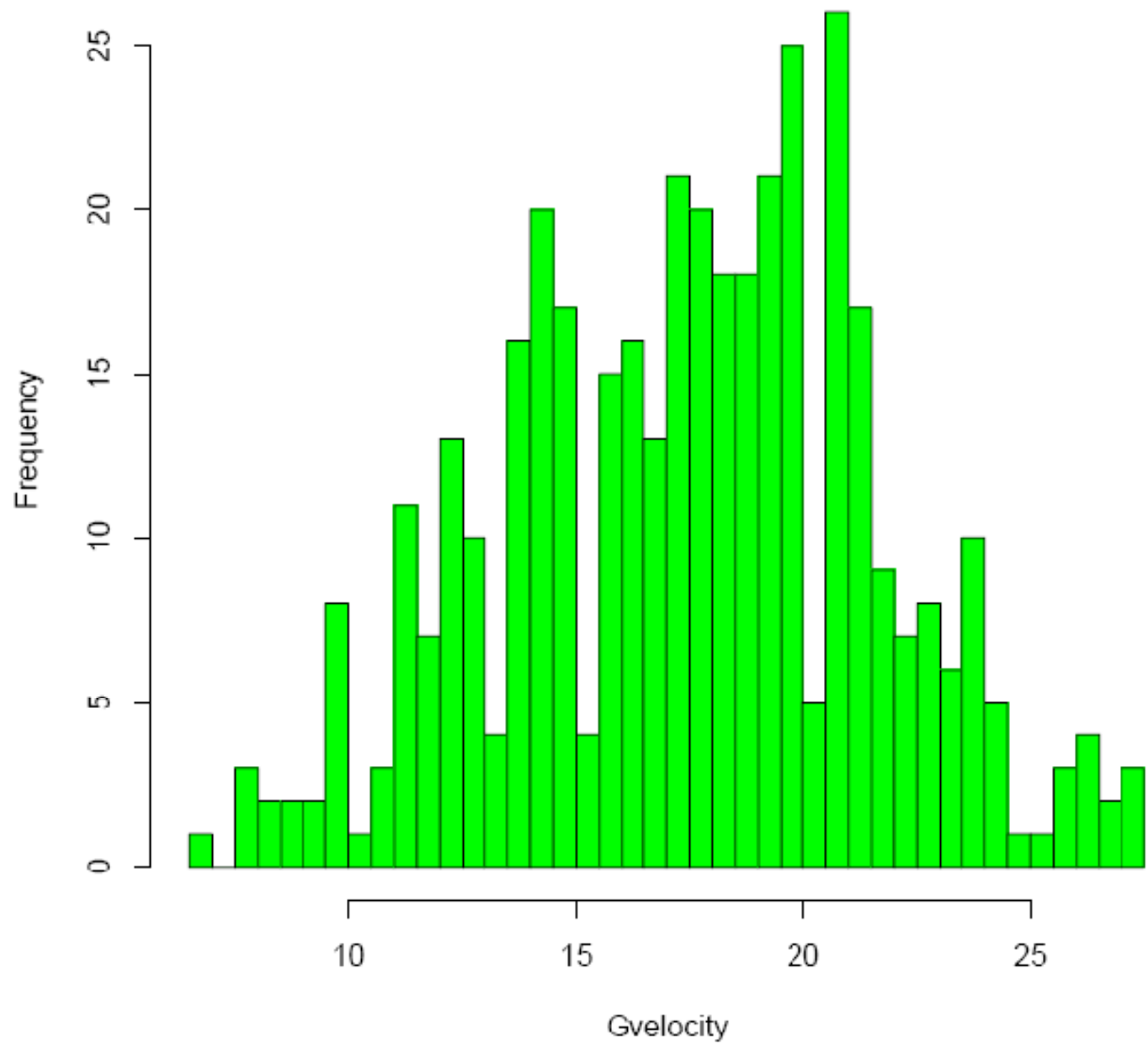
Density distribution of initial longitude of RWP (SON 1958-2008)



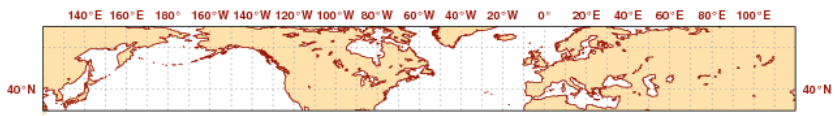
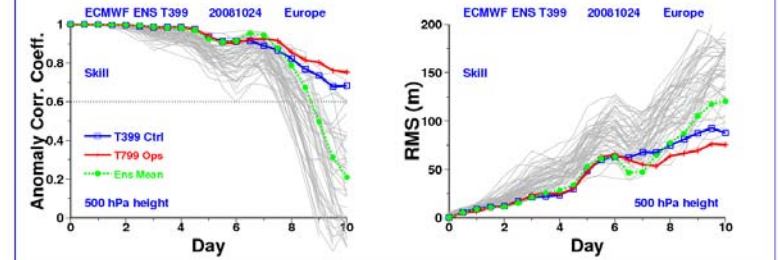
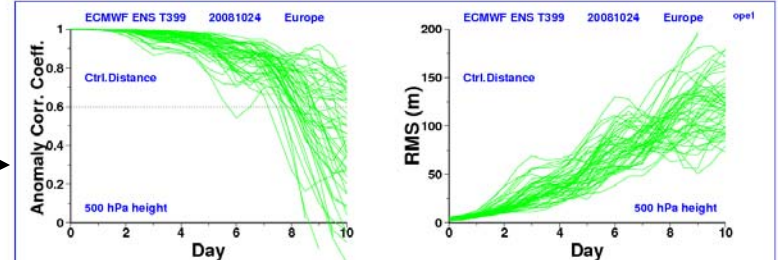
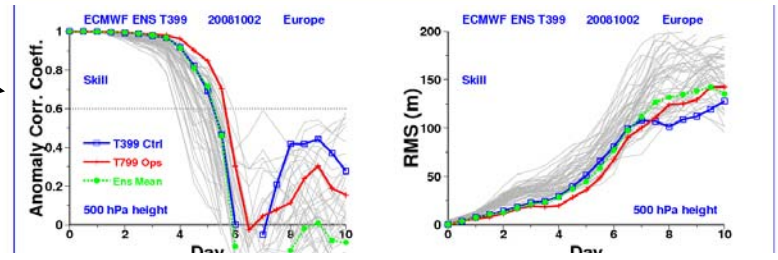
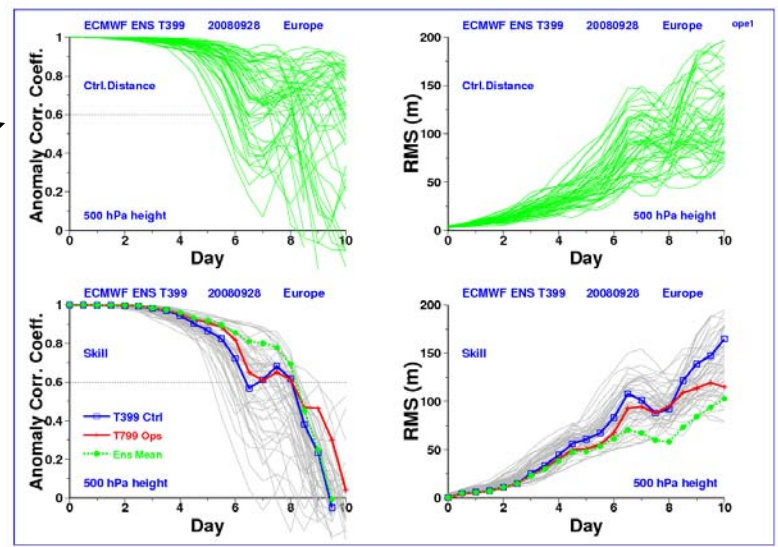
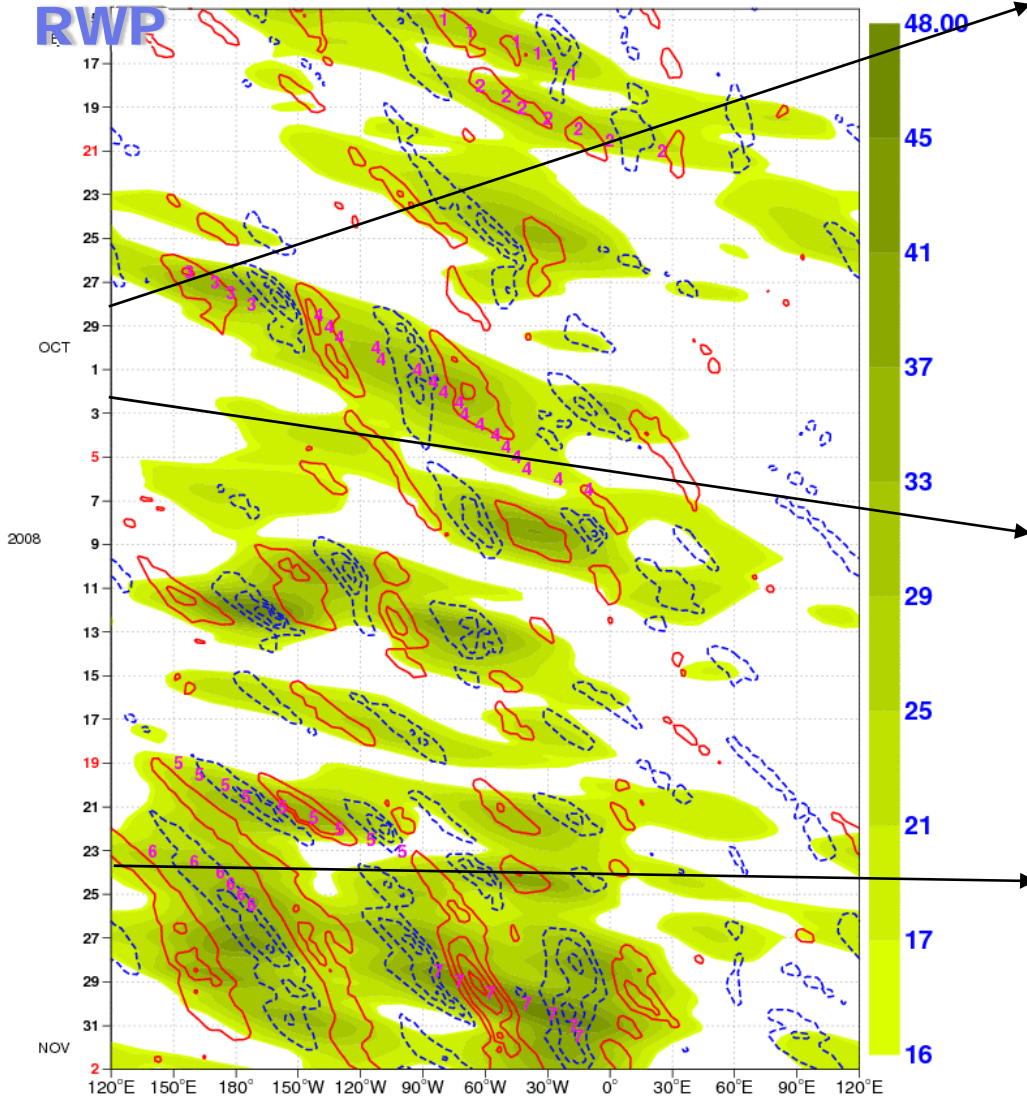
Density distribution of final longitude of RWP (SON 1958-2008)



Distribution of mean RWP velocity (SON 1958-2008)

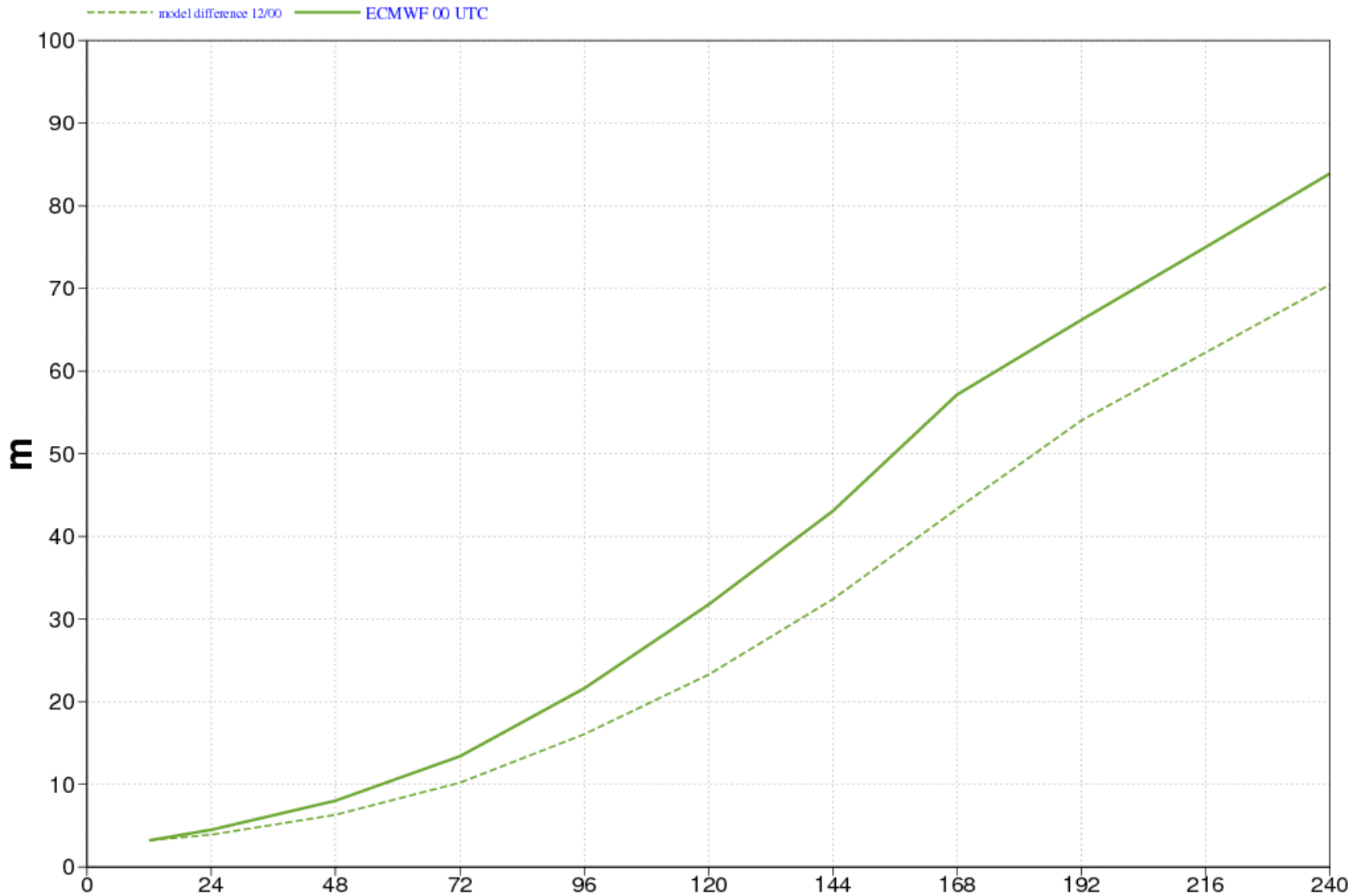


An example of EPS predictability with presence of RWP



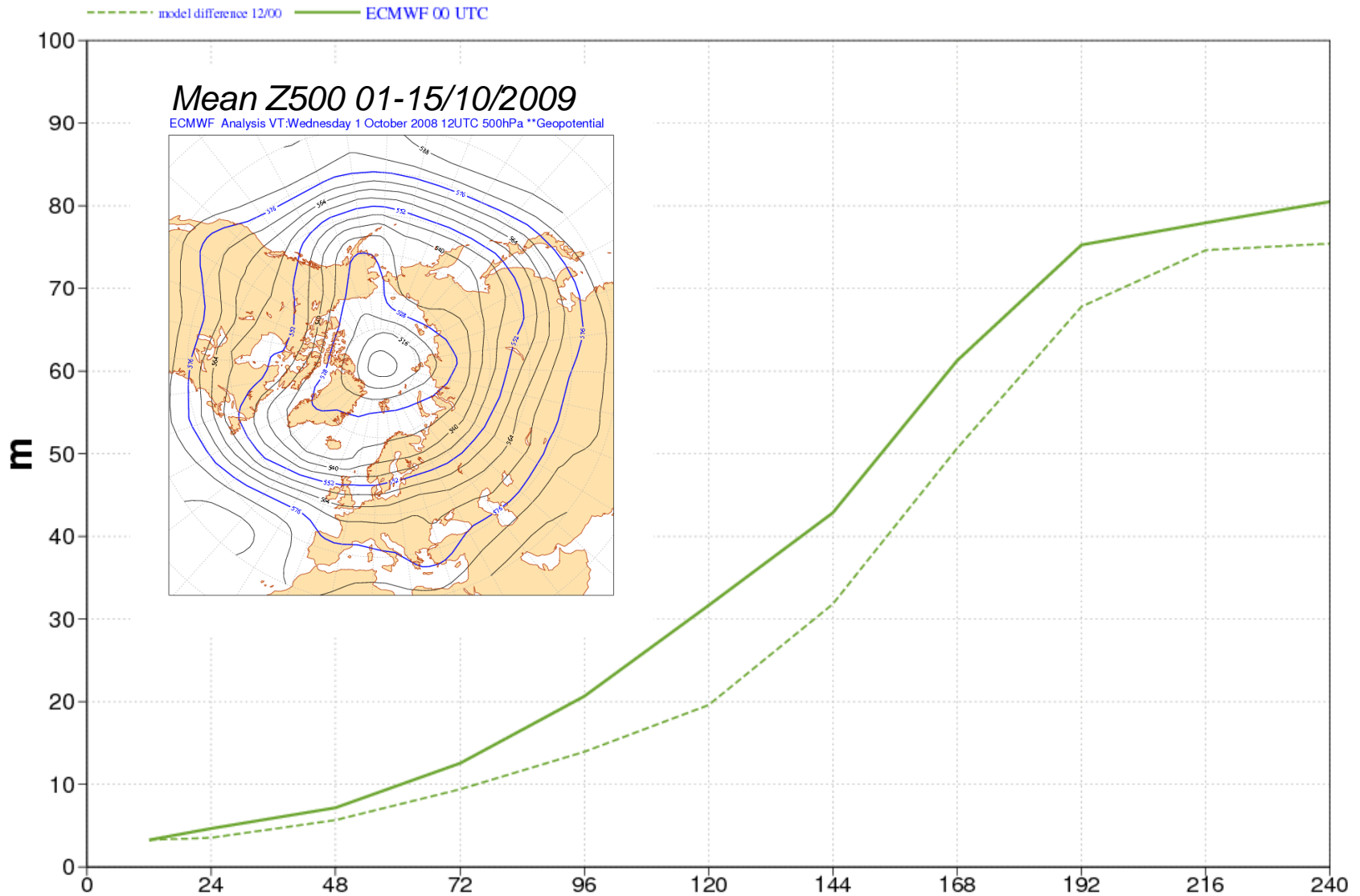
Potential predictability over Europe - Autumn

MAE and model difference Z P0500 - Periodo: 20080901_20081130



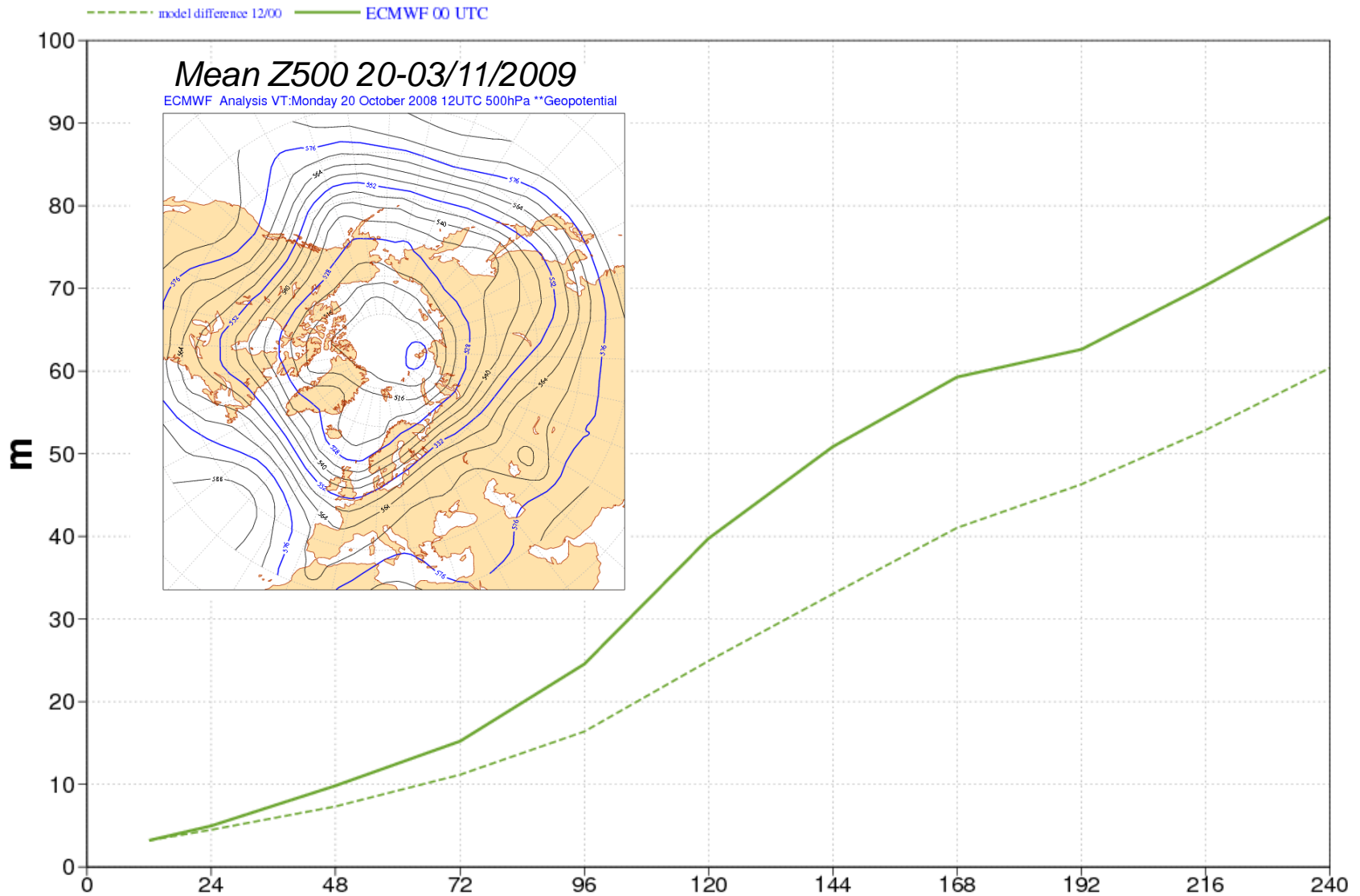
Potential predictability over Europe – Autumn/Zonal

MAE and model difference Z P0500 - Periodo: 20081001_20081015



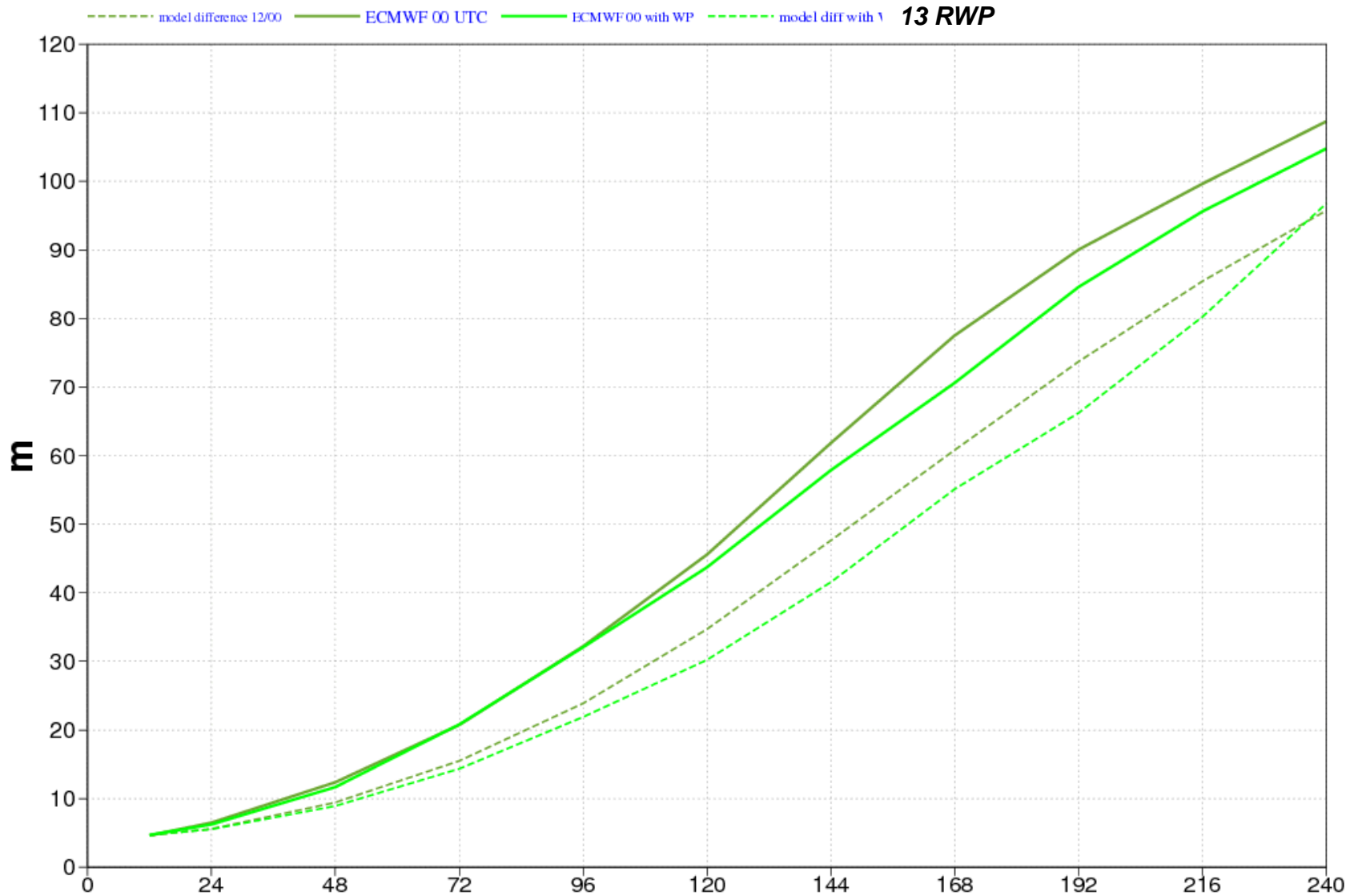
Potential predictability over Europe – Autumn/RWP

MAE and model difference Z P0500 - Periodo: 20081020_20081103



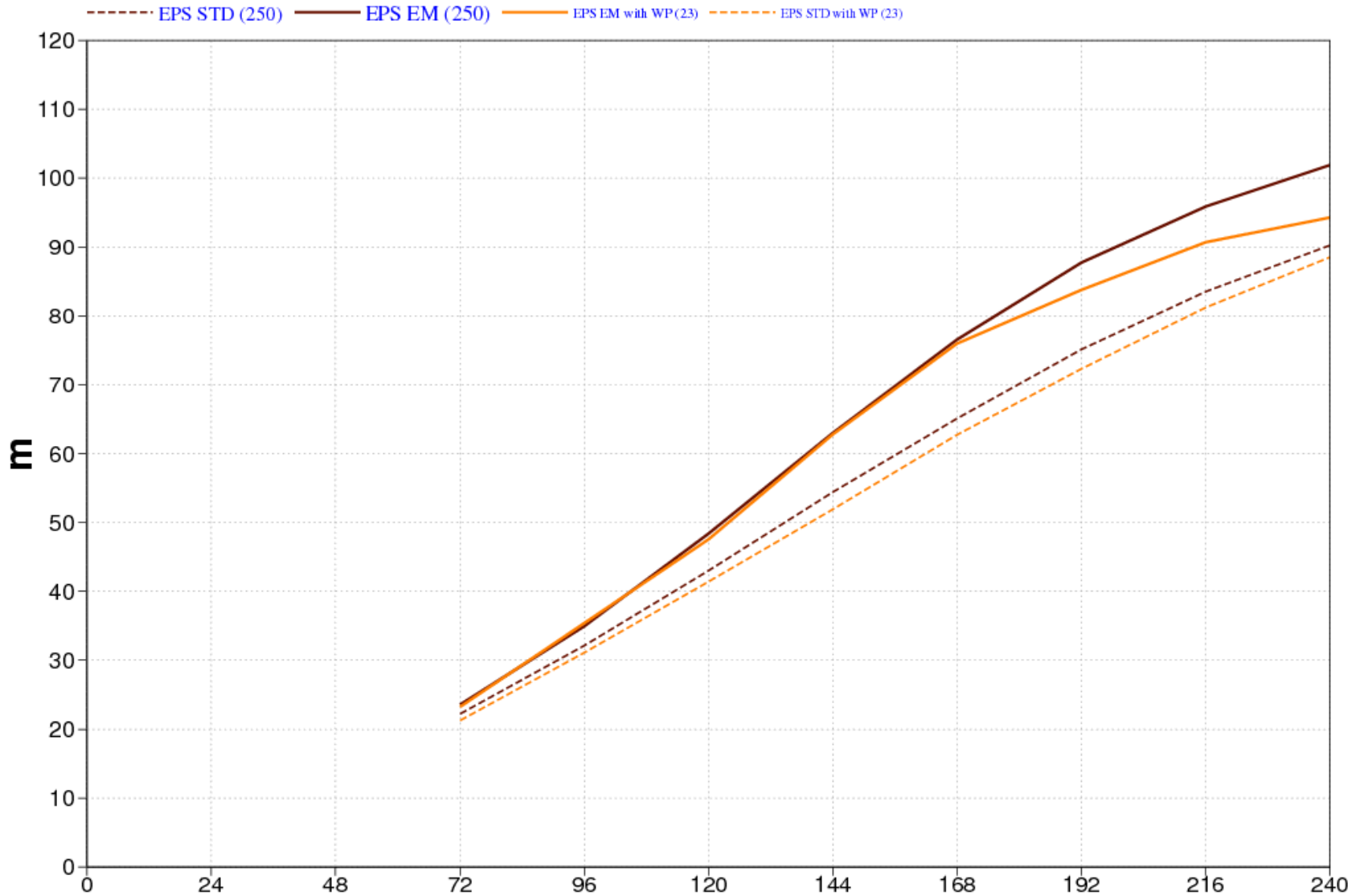
Predictability sensitivity to RWP in IC

RMSE and and RMS of model difference Z P0500 - ATL100 - Periodo: 20080901_20081231



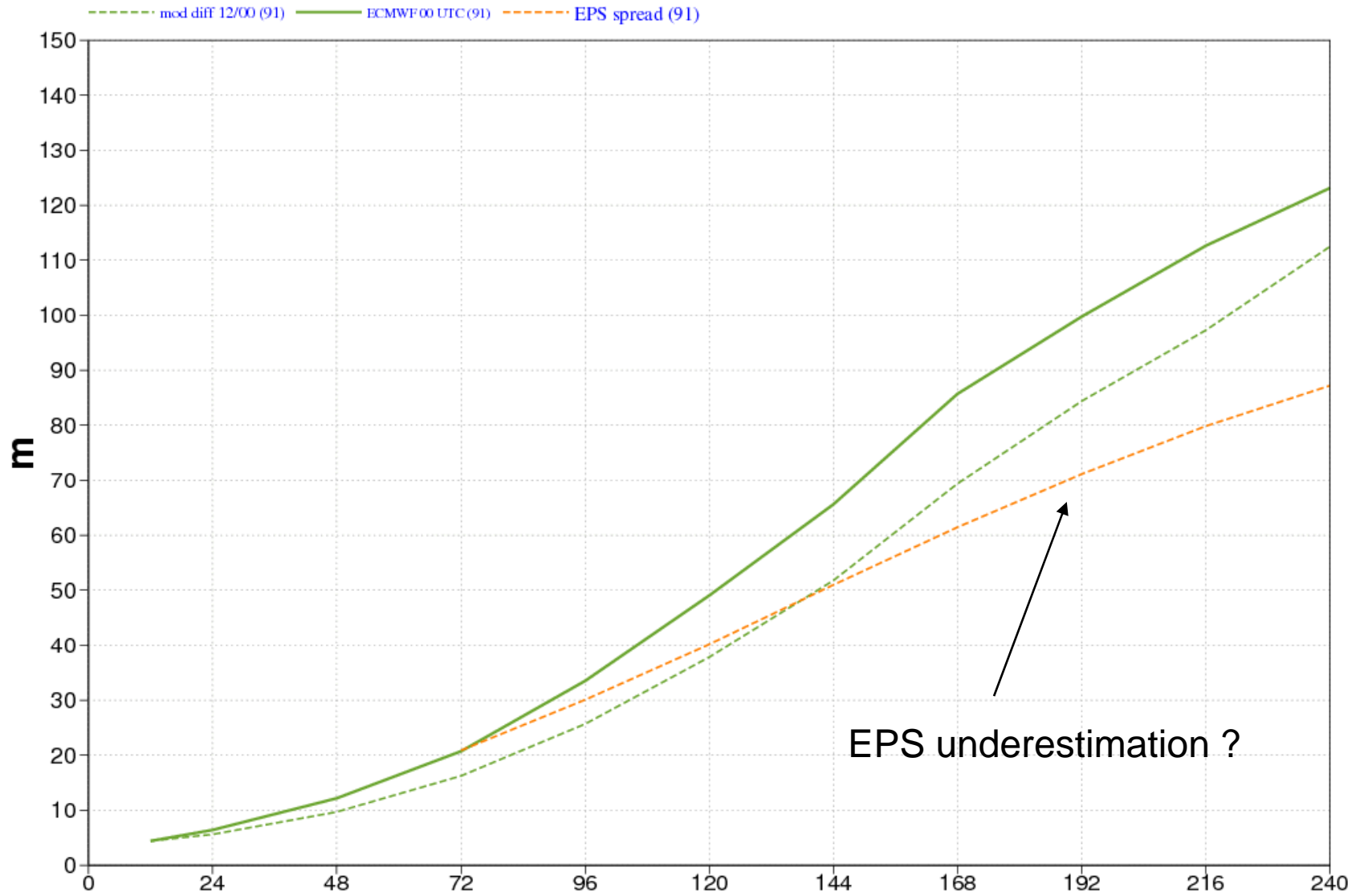
EPS predictability sensitivity to RWP in IC

EM RMSE and STD - Z500 - ATL100 - Periodo: 20080901_20090531



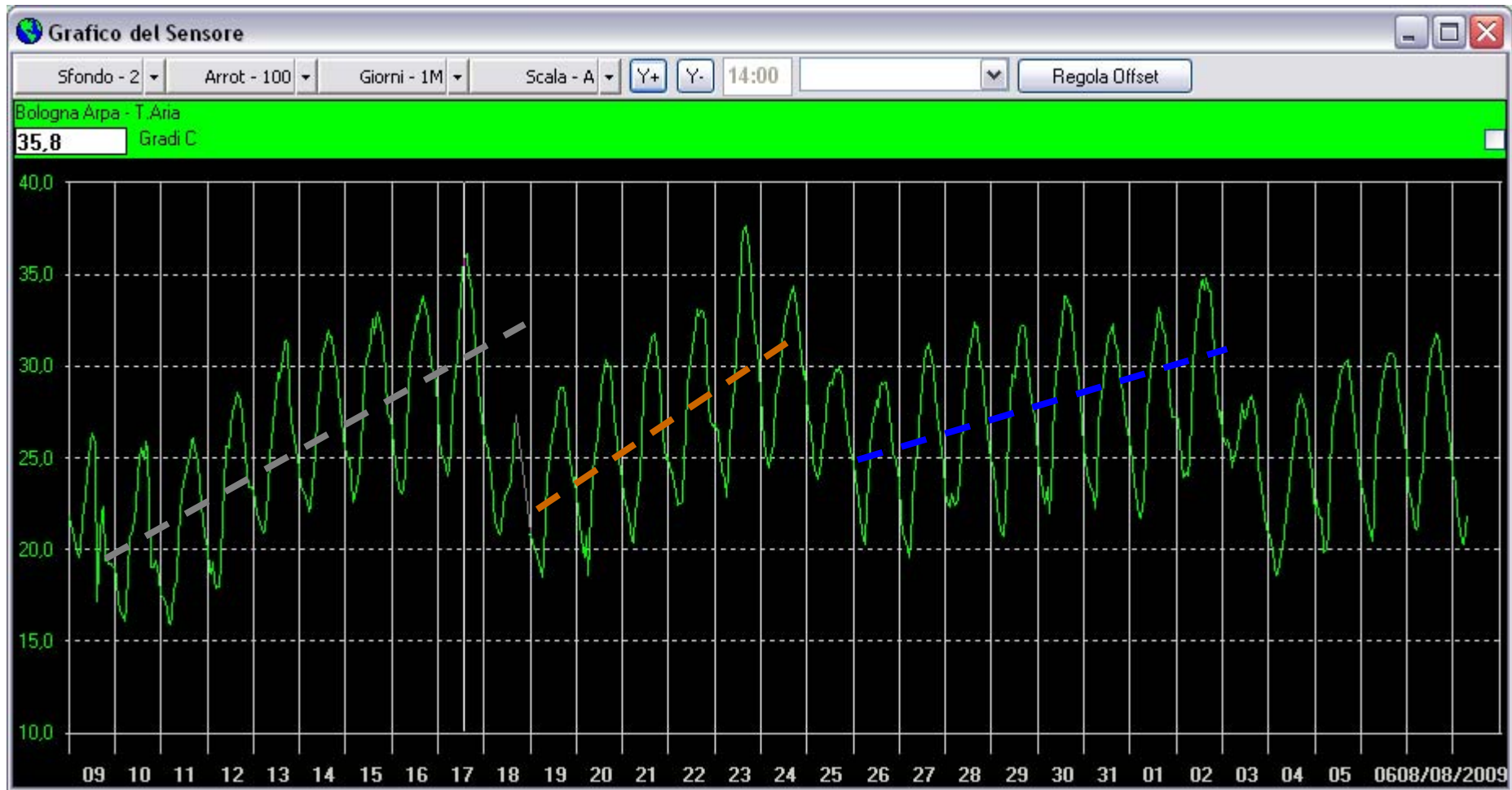
Comparison of Lorenz potential predictability and EPS Spread

RMSE and RMS of model difference Z P0500 - Europe - Periodo: 20080901_20081130



Three successive heat waves in July 2009

Daily 2m temperature observed in Bologna

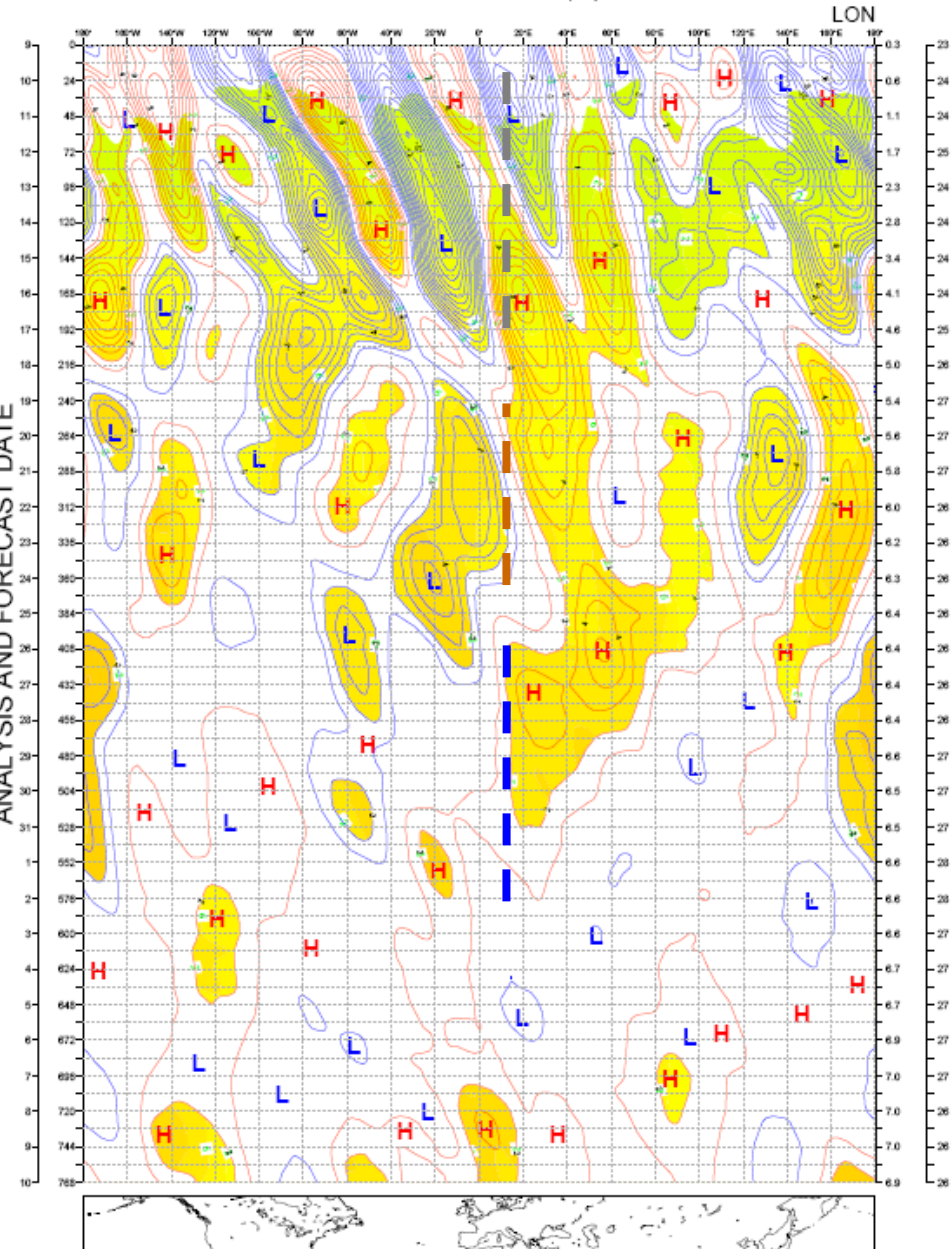


Days

HOVMOLLER DIAGRAM OF MONTHLY FORECAST 500 hPa Geopotential anomaly

09/07/2009

ENSEMBLE MEAN AND SPREAD OF 500 hPa HEIGH BETWEEN LAT 35 N AND 80 N
FORECAST BASED 9/7/2009 00UTC, Exp 1



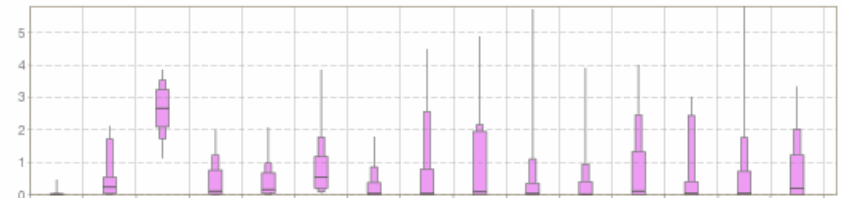
Heat waves seen by VAREPS

EPS Meteogram

Minerbio (6m) 44.56°N 11.25°E

Extended Range Forecast based on EPS Distribution Monday 13 July 2009 00 UTC

Daily mean of Total Cloud Cover (okta)



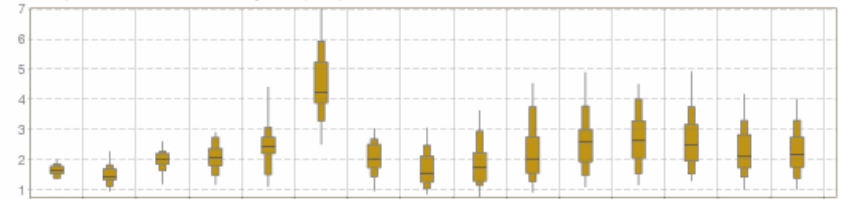
Total Precipitation (mm/24h)



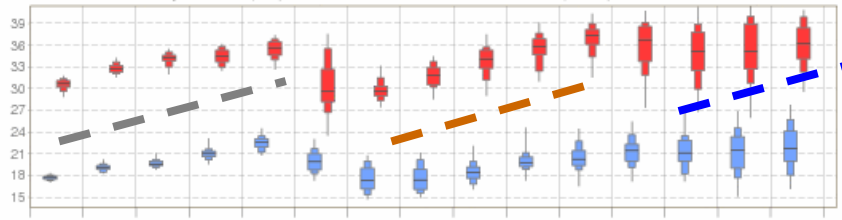
Daily distribution of 10m Wind Direction



Daily mean of 10m Wind Speed (m/s)



2m min/max temperature (°C) reduced to station height 169m (T255)



Mon 13 Tue 14 Wed 15 Thu 16 Fri 17 Sat 18 Sun 19 Mon 20 Tue 21 Wed 22 Thu 23 Fri 24 Sat 25 Sun 26 Mon 27
July 2009

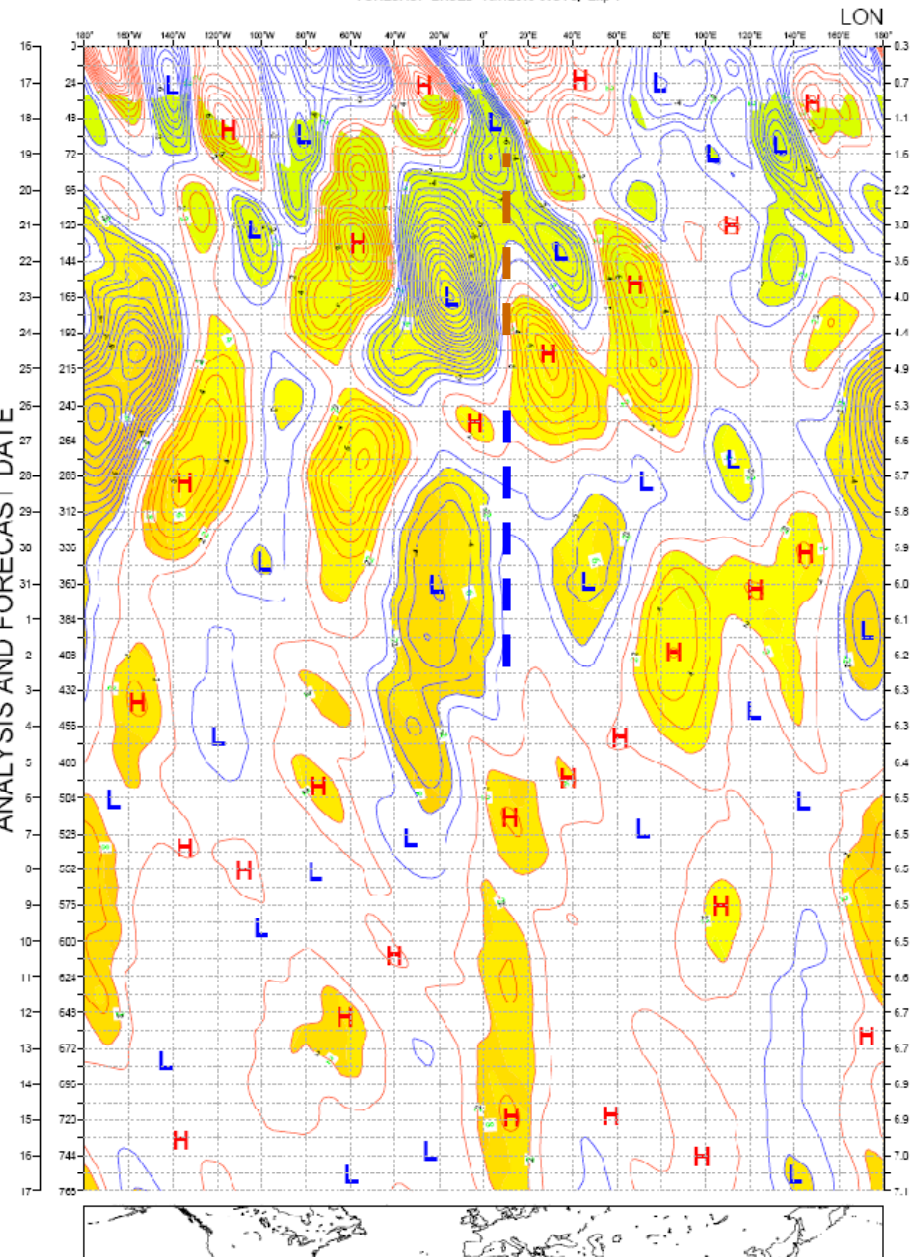
max
90%
75%
median
25%
10%
min

logics++ 2.5.7

HOVMOLLER DIAGRAM OF MONTHLY FORECAST 500 hPa Geopotential anomaly

16/07/2009

ENSEMBLE MEAN AND SPREAD OF 500 hPa HEIGH BETWEEN LAT 35 N AND 60 N
FORECAST BASED 16/7/2009 00UTC, Exp 1

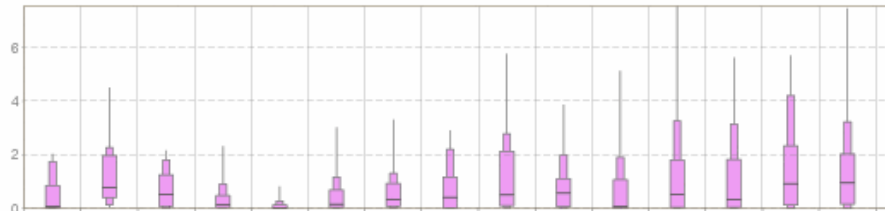


Heat waves seen by VAREPS

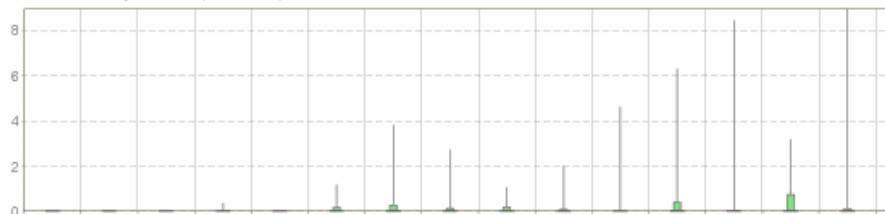
Minerbio (6m) 44.56°N 11.25°E

Extended Range Forecast based on EPS Distribution Monday 20 July 2009 00 UTC

Daily mean of Total Cloud Cover (okta)



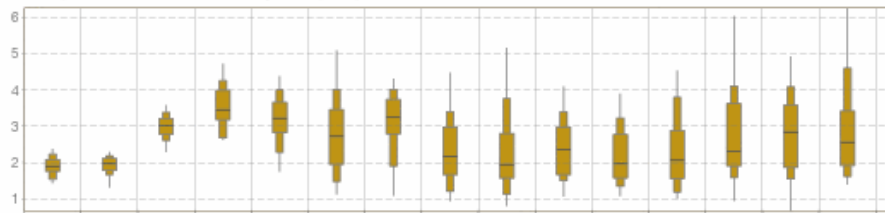
Total Precipitation (mm/24h)



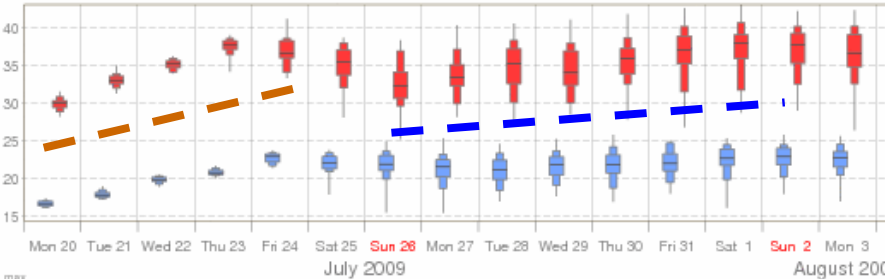
Daily distribution of 10m Wind Direction



Daily mean of 10m Wind Speed (m/s)



2m min/max temperature (°C) reduced to station height 169m (T255)



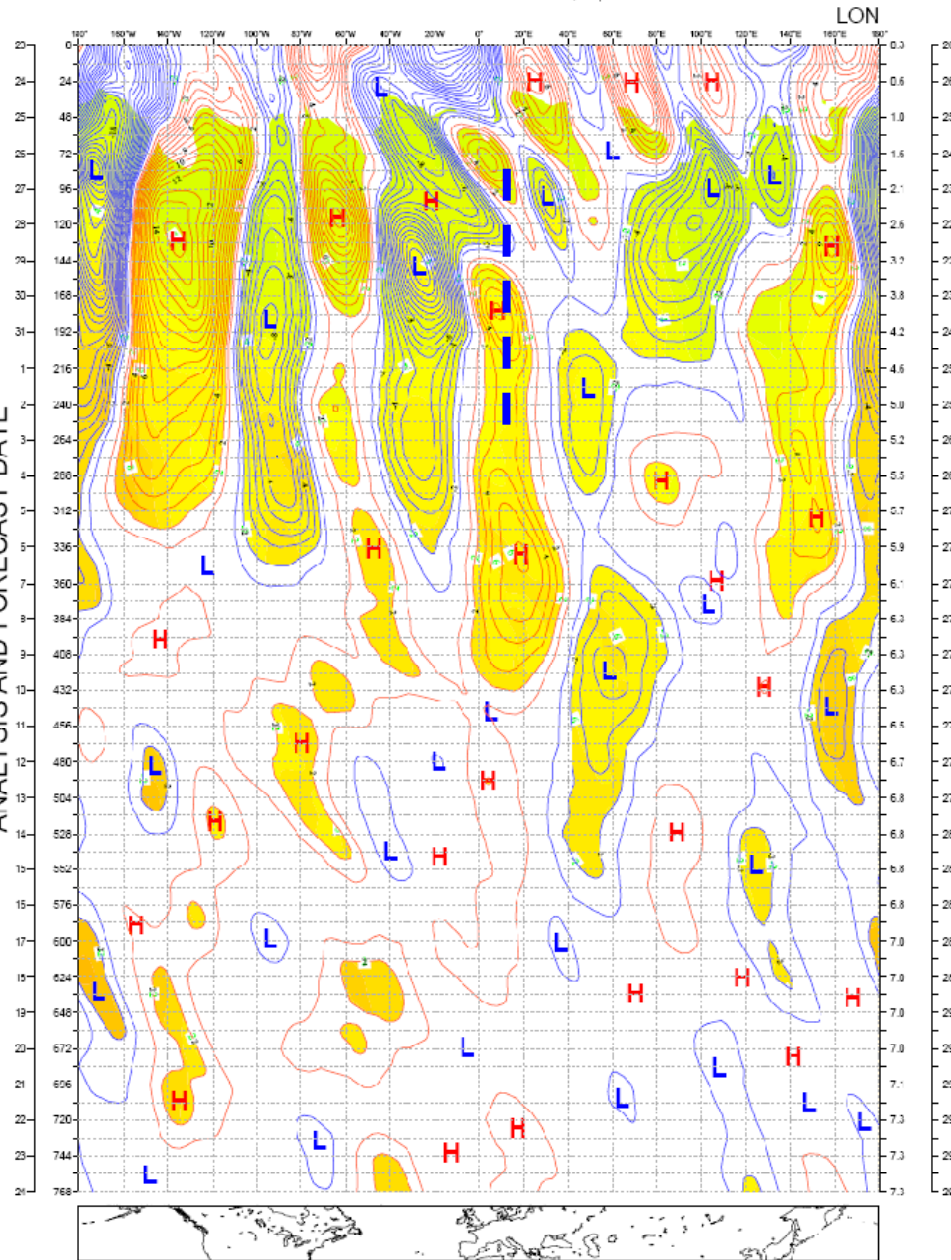
max
90%
75%
median
25%
10%
min

August 2009

HOVMOLLER DIAGRAM OF MONTHLY FORECAST 500 hPa Geopotential anomaly

23/07/2009

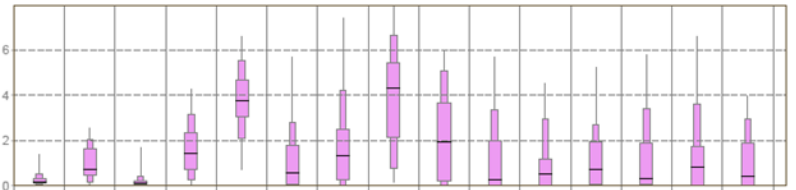
ENSEMBLE MEAN AND SPREAD OF 500 hPa HEIGH BETWEEN LAT 35 N AND 60 N
FORECAST1 BASEJ 23/7/2009 00UTC, Exp 1



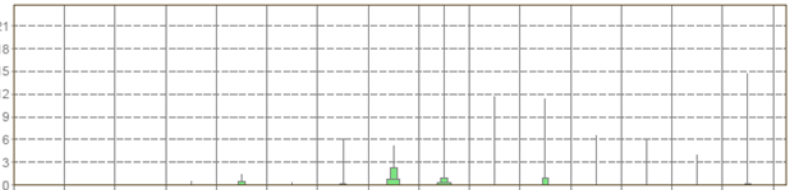
Heat waves seen by VAREPS

EPS Meteorogram
Minerbio (6m) 44.56°N 11.25°E
Extended Range Forecast based on EPS Distribution Monday 27 July 2009 00 UTC

Daily mean of Total Cloud Cover (okta)



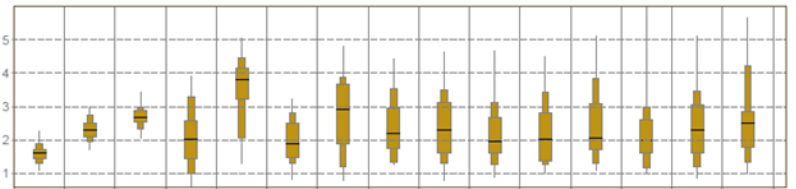
Total Precipitation (mm/24h)



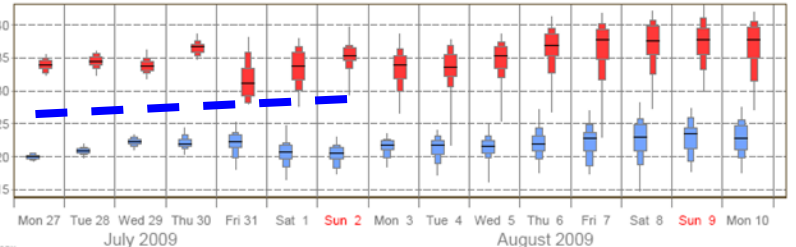
Daily distribution of 10m Wind Direction



Daily mean of 10m Wind Speed (m/s)



2m min/max temperature (°C) reduced to station height 169m (T255)



Mages++ 2.5.7

Concluding remarks (1)

We have shown impact of model changes on forecast skill, affecting in different measures forecast accuracy of different flow types.

When assessing changes in predictive skill we should always take in account of changes in predictability due to changes in the stability property of the flow. That is why we selected a local flow configuration (SSF) and we analysed the evolution of predictive skill in time

Evidence were presented indicating that spells of weather characterized by an enhanced RWP activity are more predictable than zonal conditions. In the former energy fluxes from upstream systems are dominant (Orlanski, 1995). Remote regions of the atmosphere are connected. The large-scale dynamics presents long space-time correlation. Zonal condition are characterized by synoptic transient and more localized energy exchanges.

Concluding remarks (2)

EPS estimate of predictability in RWP condition moderately support the increased predictability. Some results indicate a tendency to overestimate the spread in this situation and in general to under represent changes in predictability.

Objective RWP tracking could be proved to be a powerful tool for diagnosing core processes of large-scale dynamics like downstream development and RWP propagation in NWP and climate models. It can also be a very useful to extract valuable information from long-range forecast (ray path ensemble, clustering....)

Thank you !